Award Number: W81XWH-12-1-0380

TITLE: A Novel Locomotion-based Validation Assay for Candidate Drugs Using *Drosophila* DYT1 Disease Model.

PRINCIPAL INVESTIGATOR: Naoto Ito, Ph.D.

CONTRACTING ORGANIZATION: Massachusetts General Hospital
Boston, Massachusetts 02129

REPORT DATE: June 2014

TYPE OF REPORT: Final

PREPARED FOR: U.S. Army Medical Research and Materiel Command
Fort Detrick, Maryland 21702-5012

REPORT DOCUMENTATION PAGE

Form Approved
OMB No. 0704-0188

1. REPORT DATE	2. REPORT TYPE	3. DATES COVERED
June 2014	Final	30 September 2012-30 March 2014

4. TITLE AND SUBTITLE

A Novel Locomotion-based Validation Assay for Candidate Drugs Using *Drosophila* DYT1 Disease Model

5a. CONTRACT NUMBER
W81XWH-12-1-0380

5b. GRANT NUMBER
W81XWH-12-1-0380

5c. PROGRAM ELEMENT NUMBER

6. AUTHOR(S)

Naoto Ito, Ph.D.

E-Mail: iton@helix.mgh.harvard.edu

5d. PROJECT NUMBER

5e. TASK NUMBER

5f. WORK UNIT NUMBER

7. PERFORMING ORGANIZATION NAME(S) AND ADDRESS(ES)

Massachusetts General Hospital

Boston, Massachusetts 02129

8. PERFORMING ORGANIZATION REPORT NUMBER

9. SPONSORING / MONITORING AGENCY NAME(S) AND ADDRESS(ES)
U.S. Army Medical Research and Materiel Command
Fort Detrick, Maryland 21702-5012

10. SPONSOR/MONITOR'S ACRONYM(S)

11. SPONSOR/MONITOR'S REPORT NUMBER(S)

12. DISTRIBUTION / AVAILABILITY STATEMENT
Approved for Public Release; Distribution Unlimited

13. SUPPLEMENTARY NOTES

14. ABSTRACT

We have established fly lines expressing a mutant form of human torsinA (torsinAΔE) in fly brains. We have shown that (1) human torsinAΔE protein is expressed in fly brains; (2) expression of human torsinAΔE dominantly suppresses larval locomotion and GTPC cyclrohydolase protein levels; (3) supplementation of dopamine can partially rescue the locomotion defects of Drosophila larvae caused by the expression of human torsinAΔE. These results demonstrated that human torsinA can cause locomotion defects and reduction of GTP cyclohydrolase proteins very similar to the phenotypes in *dtorsin*-null larval brains. These results suggested that we can study the molecular defects of human torsinAΔE using our fly model system. We have submitted a manuscript describing our results. We have conducted preliminary RNAi screen to identify modifiers of dtorsin-null locomotion defect phenotype. Our preliminary results suggest that (1) dopamine signaling pathway; (2) RNP transport pathway; (3) axon guidance pathway; and (4) other early-onset dystonia genes as candidates for modifiers. These RNAi screen will be very useful for identifying potential therapeutic targets of early-onset dystonia patients.

15. SUBJECT TERMS
none provided

16. SECURITY CLASSIFICATION OF:			17. LIMITATION OF ABSTRACT	18. NUMBER OF PAGES	19a. NAME OF RESPONSIBLE PERSON
a. REPORT	b. ABSTRACT	c. THIS PAGE			19b. TELEPHONE NUMBER *(include area code)*
U	U	U	UU	33	USAMRMC

Table of Contents

	Page
Introduction……..…….…..	**4**
Body…….	**4**
Key Research Accomplishments……..	**11**
Reportable Outcomes……	**12**
Conclusion……	**14**
References……	**15**
Appendices……	**17**
Supporting Data……	**24**

"A Novel Locomotion-based Validation Assay for Candidate Drugs Using Drosophila DYT1 Disease Model"
Naoto Ito, PhD

INTRODUCTION:

Dystonia is a neurological movement disorder caused by abnormal circuitry in the brain leading to unregulated muscle contractions. It is the third most common movement disorder in humans. DYT1 is the most severe and common early-onset dystonia, resulting from a mutant form of torsinA. There are no good systems currently available for quickly validate drugs and study molecular pathways affected by the mutation using the muscle movement of whole animal as an indicator. We have proposed to develop a novel locomotion-based system for testing DYT1 drugs using *Drosophila*.

BODY: (original SOW in *italics*)

Aim 1. Develop stable fly model expressing human torsinA mutant (ΔE) and wild type torsinA in neural tissues of *dtorsin*-null Drosophila for locomotion assay.

Goal: Making a stable fly line expressing wild type htorsinA (htorA) and htorAΔE in neurons in a
Expected results: We may not be able to get high expression of transgenes. We will screen a sufficient number of transgenic lines until we obtain transgenic lines with good expression. Try different vector for making transgenes. Expression of htorADE may not produce a mobility phenotype. In that case, we will make multiple transgenic lines and examine the expression level by qRT-PCR or anti-htorA antibody. We will also try dtorsinΔE line as well.

Results:

Establishment of UAS-human torsinAΔE, UAS-Drosophila dtorsinΔE, and UAS-Drosophila dtorsinΔD transgenic lines

*dtorsin*ΔE and *dtorsin*ΔD cDNA constructs were made from the wild type *dtorsin* cDNA using QuikChange II XL Site-Directed Mutagenesis kit (Agilent Technologies, Santa Clara, CA). Briefly, a 1.2 kb wild type *dtorsin* cDNA was cut from pUAST-*dtorsin [1]* with EcoRI and NotI [1] and cloned between the EcoRI and NotI sites of pBluescript II KS (Agilent Technologies, Santa Clara, CA). Mutagenesis strand synthesis was done following the manufacture's protocol using two primers torp4aE3 (5'-CTAATGGAGGAGTTTATTATGTCAATGATTTTTTGGTTGTTCGC-3') and torp4aE5 (5'-GCGAACAACCAAAAAATCATTGACATAATAAACTCCTCCATTAG-3') to make *dtorsin* cDNA that lacks GAG (E306) (Fig. 1), and torp4aD3 (5'-CTAATGGAGGAGTTTATTATCTCAATGATTTTTTGGTTGTTCGC-3') and torp4aD5 (5'-GCGAACAACCAAAAAATCATTGAGATAATAAACTCCTCCATTAG-3') to make *dtorsin* cDNA that lacks GAC (D307) (Fig. 1) respectively. After confirming mutated sequences, the insert was again cut out with *EcoRI* and *NotI* and inserted between *EcoRI* and *NotI* sites of pUAST [2] to produce pUAST-*dtorsinΔE* and pUAST-*dtorsinΔD*. The transgenic lines E12 (pUAST-*dtorsinΔE* transgene on the second chromosome), E21 (pUAST-*dtorsinΔE* on the third chromosome) and D19 (pUAST-*dtorsinΔD* on the third chromosome) were used for the experiments.

A 1.0 kb human torsinAΔE cDNA was amplified from pcDNA3-htorM [3] by PCR using the following primers htor5 (5'-GCGGGATCCATTCATGAAGCTGGGCCGGGCCGTGCTGGGCCTGC-3') and htor3 (5'-CTCGAGCGGCCGCTCAATCATCGTAGTAATAATCTAACTTGGTG-3'). The PCR product was digested with *Acc65I* and *NotI* and inserted between *Acc65I* and *NotI* sites of pUAST [2]. Among several transgenic lines that carried a single UAS-htorsinAΔE transgene (human torsinA E302/303; Fig. 1), the transgenic line #24 with UAS-htorsinAΔE transgene on the second chromosome was used for the experiments. Injections were performed by Genetic Services, Inc. (Cambridge, MA).

Human torsinAΔE dominantly inhibits larval locomotion.

Previously, we analyzed the peristaltic frequency of third instar larvae to quantify the difference in locomotion between wild type and mutant. The wild type third instar larvae show approximately 55 muscle contraction cycles per minute when placed on 0.7% agarose plates at room temperature (22 °C). The larval movements were recorded with a movie program of a digital camera Canon Powershot G7 attached to a stereoscopic microscope. These peristaltic rates are relatively easy to score and provide a sensitive and reproducible way of quantifying larval locomotion [1,4]. Males of the *dtorsin*-null mutant, *dtorsin*^{KO13}, exhibit approximately a ~50% decrease in peristaltic rates, 22.9±2.5 (n=28, p<0.0001) (Fig. 2, column 5), compared to wild type (55.2±2.5, n=15) (Fig. 2, column 1) [1]. As previously observed, the wild type human torsinA cDNA expressed with the pan-neuronal driver elavGAL4 rescued *dtorsin*^{KO13} male larval mobility to a very significant level (56.3±3.7, n=14, p<0.0001) (Fig. 2, column 7) [1], compared to *dtorsin*^{KO13} male larvae with the elavGAL4 transgene (27.2±1.1, n=39) (Fig. 2, column 6). By way of controls, the pan-neuronal expression of the wild type human torsinA cDNA in wild type flies had no effect on larval mobility (54.3±2.3, n=15, p=0.700) (Fig. 2, column 3), compared to male larvae with elavGAL4 transgene alone (53.0±1.8, n=9) (Fig. 2, column 2). Similarly, the presence/absence of the elavGAL4 transgene had no effect on larval mobility in wild type (Fig. 2, columns 1, 2) and *dtorsin*^{KO13} (Fig. 2, columns 5, 6).

To examine the effect of mutated human torsinAΔE protein in flies, we expressed human *torsinA*ΔE cDNA with the pan-neuronal elavGAL4 driver in wild type males (*w dtorsin*$^{+}$). ElavGAL4/UAS-htorsinAΔE males exhibited a severe locomotion deficit, approaching that of the *dtorsin*-null mutant (26.7±3.4, n=9, p<0.0001) (Fig. 2, columns 2 and 4). This result demonstrates that pan-neuronal expression of human torsinAΔE protein has a negative effect on larval locomotion, similar to the *dtorsin*-null state in flies, and that it interferes with the function of endogenous Dtorsin.

While pan-neuronal expression of human wild type torsinA could rescue the locomotion deficit phenotype of *dtorsin*^{KO13} males (Fig. 2, columns 6 and 7), human torsinAΔE was unable to do so (20.5±2.0, n=21) (Fig. 2, column 8). To determine whether the human torsinAΔE could inhibit wild type human torsinA, we co-expressed the human torsinAΔE cDNA with the wild type human torsinA cDNA in *dtorsin*^{KO13} male using the same elavGAL4 driver. Co-expression of human wild type torsinA and human torsinAΔE resulted in a significant inhibition of mobility (25.3±2.8, n=14, p<0.0001) (Fig. 2, column 9) compared to the rescue by human torsinA alone (Fig. 2, column 7).

Human torsinAΔE dominantly suppresses GTPCH expression.

We have previously shown, and confirm here, that *dtorsin*^{KO13} males have a severe reduction of both the 45kD (Pu-RA) and 43kD (Pu-RC) isoforms of GTPCH protein in adult brains (Fig. 3, lane 1 and 2) [1]. To investigate whether human torsinAΔE has a similar effect on GTPCH, we prepared extracts from heads of *dtorsin*^{KO13} adult males expressing human torsinAΔE in neurons, *dtorsin*^{KO13} adult males expressing wild type torsinA in neurons, and *dtorsin*^{KO13} adult males expressing both human torsinA and human torsinAΔE in neurons, and compared GTPCH protein levels by western blot analysis (Fig. 3, lane 3-5). Pan-neuronal expression of human torsinAΔE in *dtorsin*^{KO13} adult males, confirmed by immunoblotting using an antibody specific to human torsinA [5] (Fig. 4, lanes 1 and 4), revealed that the mutant human torsinA protein reduced GTPCH protein levels even further than those of *dtorsin*^{KO13} adult males to an undetectable level in the case of Pu-RC isoform (Fig. 3, lane 3). Neuronal expression of human torsinA (Fig. 4, lane 3) strongly rescued the Pu-RC isoform of GTPCH of *dtorsin*-null males (compare Fig. 3, lanes 2 and 4). Severe reduction of GTPCH was observed in *dtorsin*^{KO13} adult males expressing human torsinA and human torsinAΔE together (compare Fig. 3, lanes 2 and 5), even though the expression of torsinAΔE with the wild type form does not diminish the levels of human torsinA expressed in fly neurons (Fig. 4, lane 5). We obtained comparable results using brain extracts from third instar larvae of the corresponding genotypes (data not shown) as those of adult head extracts. These results confirm that wild type human torsinA is capable of rescuing neuronal expression of *Drosophila* GTPCH and demonstrate that the human torsinAΔE, when co-expressed with the wild type human transgene, dominantly suppresses GTPCH

protein levels in both larval and adult brains without negatively affecting the expression of wild type human torsinA.

DtorsinΔE dominantly inhibits larval locomotion.

Dtorsin protein has conserved amino acids E306/D307, compared to E302/E303 in human torsinA (Fig. 1). To determine whether Dtorsin with either ΔE306 or ΔD307 deleted would have a similar dominant-negative activity on the wild type Dtorsin protein as observed for the human torsinAΔE302/303 mutation, we made two deletion mutant constructs of the *dtorsin* cDNA in E306 (UAS-*dtorsinΔE*) and D307 (UAS-*dtorsinΔD*) and expressed them with the elavGAL4 driver. Although pan-neuronal expression of wild type Dtorsin did not affect larval locomotion in wild type *Drosophila* (peristaltic frequency 53.0±1.5, n=8, not significant) (Fig. 5, column 2) compared to wild type (53.0±1.8, n=9) (Fig. 5, column 1), wild type male larvae expressing DtorsinΔE exhibited a significant locomotion deficit (38.7±2.5, n=23, p=0.002) (Fig. 5, column 3). Male larvae co-expressing DtorsinΔE and wild type Dtorsin also exhibited a locomotion deficit (38.54±2.8, n=15, p=0.0012) (Fig. 5, column 4 compared to column 1) similar to the deficit caused by expression of DtorsinΔE only (column 3).

Mutant male larvae (*dtorsin*^{KO13}) expressing wild type Dtorsin showed much improved larval locomotion. We tested two independent transgenic lines to express wild type Dtorsin. Expression of a second chromosome transgene, UAS-*dtorsin*(B5) in male *dtorsin*^{KO13} larvae resulted in a peristaltic frequency of 50.5±2.5, n=20, p<0.0001 (Fig. 5, column 6), while expression of another transgene UAS-*dtorsin*(A11), on the third chromosome, rescued the peristaltic frequency to 48.2±1.1, n=9, p<0.0001 (Fig. 5, column 7) compared to the *dtorsin*-null (*dtorsin*^{KO13}) males (Fig. 5, column 5). Expression of UAS-*dtorsin*(B5) and UAS-*dtorsin*(A11) together in the *dtorsin*-null background did not elevate locomotion further (peristaltic frequency: 50.2±1.2, n=23, p<0.0001) (Fig. 5, column 8).

In striking contrast to the rescuing effect of wild type Dtorsin expression, DtorsinΔE expression in male *dtorsin*^{KO13} larvae failed to rescue the locomotion deficit (22.9±2.8, n=13, not significant) with a slight reduction of peristaltic rate (Fig. 5, column 9), relative to *dtorsin*^{KO13} males (Fig. 5, column 5). Similarly, mutant males co-expressing DtorsinΔE and wild type Dtorsin transgenes exhibited a locomotion deficit that was not significantly different from that of the *dtorsin*^{KO13} larvae (UAS-*dtorsin*(A11) and UAS-*dtorsin*ΔE(#12); 32.4±4.2, n=7, not significant) (Fig. 5, column 11); UAS-*dtorsin*(B5) and UAS-*dtorsin*ΔE(#21): 29.9±3.6, n=14, not significant) (Fig. 5, column 12).

Interestingly, pan-neuronal expression of DtorsinΔD in *dtorsin*^{KO13} males rescued the larval mobility (45.2±2.9, n=11, p<0.0001) (Fig. 5, column 10 compared to column 5). Similarly, co-expression of DtorsinΔD with the wild type Dtorsin in *dtorsin*^{KO13} males had no effect on locomotion (peristaltic frequency: 49.4±3.2, n=20) (Fig. 5, column 13). These results indicate that E302/303 of human torsinA protein and E306 of *Drosophila* Dtorsin protein are functionally similar and that deletion of these glutamates both cause reduced locomotion in *Drosophila* larvae, presumably due to the same functional abnormality.

DtorsinΔE dominantly suppresses GTPCH expression.

These studies described above demonstrate a striking similarity in the dominant inhibition of larval locomotion by DtorsinΔE and human torsinAΔE. Since we found that human torsinAΔE dominantly inhibited GTPCH protein expression, we next examined the protein levels of GTPCH in adult male heads expressing wild type Dtorsin and DtorsinΔE in the *dtorsin*-null background (Fig. 6). The expression of endogenous Dtorsin in the *dtorsin*$^{+}$ parental line (Fig. 6, lane 1) and in the *dtorsin*$^{+}$ elavGAL4 transgene line (Fig. 6, lane 2) revealed similar patterns of GTPCH expression, although somewhat reduced levels, likely due to genetic background differences. Dtorsin expressed in *dtorsin*^{KO13} males, under the control of elavGAL4, rescued GTPCH expression substantially (Fig. 6, lanes 5, compared to lanes 3 and 4). As we observed when the wild type human torsinA was expressed using elavGAL4, the wild type Dtorsin transgene rescued the Pu-RC isoform of GTPCH only. As is the case when human torsinA protein is expressed, the non-rescued GTPCH isoform is

most likely non-neuronal, and therefore not affected by neuron-specific expression of the transgenes by elavGAL4.

DtorsinΔE expressed in *dtorsin*^{KO13} neurons failed to affect the GTPCH protein level (Fig. 6, lane 6, compared to lane 3). Severe reduction of GTPCH was also observed in adult males co-expressing Dtorsin and DtorsinΔE in *dtorsin*^{KO13} (Fig. 6, lane 7). These results demonstrated that DtorsinΔE and human torsinAΔE have indistinguishable effects on the expression of GTPCH protein in *Drosophila* brains, both dominantly inhibiting GTPCH expression.

The mobility defect of larvae expressing either human torsinAΔE or DtorsinΔE can be rescued by dopamine supplementation.

In *Drosophila*, ingestion of dopamine increases dopamine pools in the fly head, though in mammals peripheral dopamine does not enter the brain [6]. We previously showed that the locomotor deficit phenotype in *dtorsin*^{KO13} mutant male was restored by dopamine supplementation to the larval growth medium, but not by serotonin or octopamine [1]. Since we observed in the current study a very similar reduction of dopamine levels in larval brains expressing human torsinAΔE, we hypothesize that dopamine supplementation to the larval growth medium could also restore the locomotion defect of larvae expressing human torsinΔE (or *Drosophila* DtorsinΔE). To test this hypothesis, we added 20mM dopamine in the food of larvae with different *dtorsin* genotypes (Fig. 7). Dopamine supplementation rescued the locomotion defect of *dtorsin*^{KO13} larvae expressing DtorsinΔE and wild type Dtorsin (51.4±2.6, n=8, $p<0.0001$) (Fig. 7, column 2) compared to the larvae of the same genotype without dopamine (25.9±2.5, n=11) (Fig. 7, column 1). Similarly, dopamine supplementation also rescued the locomotion defect of *dtorsin*^{KO13} larvae expressing human torsinΔE and wild type torsinA (52.2±3.6, n=5, $p<0.0001$) (Fig. 7, column 4) compared to the larvae of the same genotype without dopamine (25.3±2.8, n=14) (Fig. 7, column 3). These results demonstrate that locomotor defects caused by the pan-neuronal expression of human torsinAΔE or DtorsinΔE can be rescued by dopamine supplementation.

Aim 2. Optimize drug feeding conditions and locomotion assay for accurate and efficient quantification of effects, and test candidate drugs in established system.

Goal: Optimize the drug feeding condition and mobility assay protocol.
Expected results: In order to minimize the amount of drugs required for assays, we wanted to minimize the food and water. Optimize the size of the fly vials, number of larvae in one tube, length of drug feeding, and concentration of drugs. The mobility assay is rather tedious and time consuming. Doing mobility assays for dozens of larvae requires considerable effort. We need to decrease the number of larvae required for one drug as much as possible.

Results:
Standard assay condition

We currently use narrow *Drosophila* vials (25 x 95mm; Catalog number #32-116) purchased from Flystuff/Genesee Scientific (San Diego, CA) when we add drug solutions to the culture medium. The dopamine feeding assay described above was done with some modification as described previously [1]. Fifty females of *w, elavGAL4, dtorsin*^{KO13}*/FM7i*, *Actin-GFP* were mated with twenty-five males of *w*; UAS-*dtorsin*(A11)(II);UAS-*dtorsin*ΔE(12)(III) or *w*; UAS-htorsinA(#8), UAS-htorsinAΔE(#24)(II). Fifty Green Fluorescent Protein (GFP)-negative first instar larvae were transferred to 1.5 g Formula 4-24 Instant Drosophila Medium (Carolina Biological Supply Company, Burlington, SC) in 7 ml water or 7 ml of 20 mM dopamine hydrochloride (Sigma-Aldrich) solution. Larval locomotion assays were performed as described at the wandering stage of third instar [1].

For this standard condition, we need 7 ml of water or drug solution during the larval growth. We tested smaller amount of water volume (5 ml or less) with smaller amount of medium, but the

larvae became too unhealthy and we could recover much less 3rd instar larvae. We tested smaller vials with much less recovery rate. We tested 16 x 95 mm flat bottomed tubes (Globe Scientific Inc. Catalogue #115055) and 16.5 x 95 mm flat bottomed tubes (Sarstedt Catalogue #58.941) with similarly poor results. These tubes had diameters too small for fully-grown larvae to move around. We concluded that it is difficult to decrease the amount of medium plus water we use to obtain consistent results.

As described, we typically use 50 larvae for one vial when we grow them. When we have fewer than 50 larvae, the recovery rate of third instar larvae were much decreased, while we could increase up to 100 larvae without overcrowding. As long as we keep these conditions, the peristaltic rates of larvae were pretty consistent (data not shown). When the density of larvae are too low in the tubes, the medium tend to become too dry which is not good for larvae to grow. We concluded that it is difficult to decrease the numbers of larvae or use smaller vials for conducting these locomotion assays to obtain reliable results.

Aim 3. Screen RNAi transgenic lines in the established locomotion system to identify new potential drug targets.

Expected results: Some of the RNAis may cause lethal or toxic effects alone. In order to avoid this problem, we will test their effect first by expressing them in the wild type. Some of the RNAi may have off-target effects. For the ones that showed modulation of mutant torsinA in mobility assay, test multiple RNAi lines targeted to the same gene if they are available. Examine the effectiveness of RNAi on target mRNA by qRT-PCR.

Results:

Identification of genes and pathways that could modify *Drosophila* dtorsin mutant deficits by expressing RNAi in neurons.

We proposed to use RNA interference technology to screen genes that are on the dtorsin signaling pathways. The *Drosophila* system is very useful for systematically identifying genetic modifiers of *dtorsin*-null phenotypes. More than 20,000 fly lines have been created and distributed from the two different stock centers (Drosophila RNAi Screening Center at Harvard Medical School: www.flyrnai.org, and Vienna Drosophila RNAi Center: http://stockcenter.vdrc.at/control/main) with more than 95% of the *Drosophila* genes being represented. These transgenic lines can express short or long hairpin loops (RNAis) for different genes using UAS-GAL4 expression system and down-regulate specific mRNAs [7-9]. The hairpin constructs were inserted at the same location on the genome using the same parental fly line, minimizing the effect of surrounding sequences and genetic variations on the expression of the RNAi transgenes.

We made a fly line with *dtorsin*-null gene (on the X-chromosome) with a pan-neuronal promoter elavGAL4 (on X) over GFP-marked balancer X-chromosome (*w*, *elavGAL4*, $dtorsin^{KO13}$/FM7i, Act-GFP) [1]. Dtorsin-null larvae can be easily distinguished from wild type larvae by the absence of GFP fluorescence. Females of *w*, elavGAL4, $dtorsin^{KO13}$ / FM7i, Act-GFP were mated with males of RNAi lines. GFP-negative progeny was selected at the first instar stage and peristaltic rates were determined at the late third instar stage as described previously [1]. Since *dtorsin* gene is on the X-chromosome, all the GFP-negative males are *dtorsin*-null hemizygotes expressing RNAi in neurons (*w*, *elavGAL4*, $dtorsin^{KO13}$ / Y; UAS-RNAi/+), while all the GFP-negative females are *dtorsin*-null heterozygotes expressing RNAi in neurons (*w*, *elavGAL4*, $dtorsin^{KO13}$ /+; UAS-RNAi). We did not observe any difference in peristaltic rates between males and females (data not shown). Since dtorsin-null mutation is male-sterile, we could not get homozygous females [1].
Five to ten larvae for each genotype were assayed to calculate average peristaltic rates per min.

We have tested 150 RNAi lines so far and the results for 28 RNAi lines are shown in Fig 8. *Dtorsin*-null hemizygote male larvae show severely reduced peristaltic rates without RNAi (~30

cycles/min) (Fig 8 column1), indicating the presence or absence of elavGAL4 driver did not have any effect on larval locomotion. *Dtorsin*-null heterozygote female larvae showed no apparent reduction of peristaltic frequencies without RNAi (Fig 8 lane1), although they have substantially reduced GTPCH protein and dopamine levels [1]. Neural expression of RNAi #2, #4, #5, #7, #12, #13, #14, #15, #16, #18, #19, #23, or #24 had no effect in either males or females (Fig 8). Neuronal expression of RNAi #6, #9,or #20 had no effect in *dtorsin*-null heterozygous female larvae (Fig 8), while they strongly suppressed peristaltic rates to the level very close to the wild type rate (55-60 cycles/min) ($p<0.0001$). RNAi #6, #9, #20 are candidates for strong "suppressors" of *dtorsin*-null locomotion defects. Neuronal expression of RNAi #8 weakly suppressed *dtorsin*-null locomotion defects (Fig 8).

Neuronal expression of RNAi #10, #11, #21, or #22 in *dtorsin*-null heterozygous female larvae (Fig 8) strongly decreased peristaltic rates to ~30, a rate which is very close to those of the *dtorsin*-null male larvae, while no effect was observed in males (Fig 8). These are candidates for strong "enhancers" of *dtorsin*-null locomotion defects. RNAi #3, #26, #27, #28, and #29 are candidates of weak enhancers.

Neuronal expression of RNAi #25 decreased peristaltic rates both in *dtorsin*-null hemizygous males and *dtorsin*-null heterozygous females. Line #25 has RNAi for *shibire* gene encoding dynamin, which is required for endocyctosis [10,11]. Mutation in *shibire* gene is known to block endocytosis and was reported to have depletion of synaptic vesicles [10]. This is an example of RNAi whose expression causes general inhibition of locomotion rather than specific modification of torsin signaling pathway. We have found very few examples of these RNAi that showed general inhibition of locomotion.

We have tested150 RNAi lines so far, mainly focusing on (1) neurotransmitter signal transduction pathways, (2) RNP transport pathways, (3) cell migration and axon guidance pathways, and (4) other dystonia genes. We can routinely assay 2-3 lines per week and total of 100-150 lines per year. For one genotype, we routinely counted 5-10 males and females for each RNAi line that give us statistically significant results. Larval locomotion was recorded for 1 minute using a Canon Powershot G7 digital camera attached to a stereoscopic microscope. The peristaltic rates of the control and test line were compared pair-wise to the control without RNAi by an unpaired T-test using Prism 5 software (Graphpad).

RNAi lines for each gene are listed in flybase (flybase.org). Although there are two major sources of the RNAi lines, we will initially obtain RNAi transgenic lines from the Drosophila RNAi Screening Center (Harvard University Medical School), distributed through the Bloomington Drosophila Stock Center (Indiana University). There are more than 2,600 lines currently available with more lines being produced from them. This is a cheaper ($1-2/line) and more convenient source of RNAi lines for US researchers. Vienna Drosophila RNAi Center, in Vienna, Austria, has over 20,000 fly RNAi lines with more than 95% of genes represented. Theirs are much more expensive (~$20/line) and requires special import permit from USDA. We used Vienna fly RNAi lines as a secondary source when there are no RNAi lines available from the Bloomington Stock Center for that gene.

Our screen has so far identified multiple candidate modifier genes of *dtorsin*-null locomotion phenotype and these genes can be classified into three major categories, (1) genes in dopamine signaling pathway, (2) genes in RNP transport pathway, and (3) genes in axon guidance and cell migration pathway (Table 1).

(A) Dopamine signaling pathway

Many of the strongest "suppressor" and "enhancer" lines are found in genes that regulate dopamine pools (DAT: Dopamine transporter (Fig 8 column 6) and Punch: GTPCH (Fig 8 column 3)) and genes in dopamine signaling pathway (DopR2: Dopamine D1 receptor (column 9), Gαs: G protein α s subunit/GNAL ortholog (column 20), D2R: Dopamine D2 receptor (column 10 and 11), Gαq: G protein α q subunit (column 21), and Gαi: G protein α I subunit (column 22)). These results are consistent with a hypothesis that *dtorsin*-null larval brains have reduced dopamine synthesis and impaired D2 receptor signaling. Knocking-down of DAT would decrease DA uptake into neurons, resulting in decreased synaptic dopamine concentration [12] and could rescue the dopamine

depletion caused by reduced GTPCH protein levels. Knocking-down of dopamine D1 receptor would decrease signaling through D1 receptor, thus restoring the unbalance between D2 receptor and D1 receptor signaling caused by impaired D2 receptor signaling. Among G proteins we have tested, Gαi and Gαq are believed to be coupled to dopamine D2 receptor, while Gαs is coupled to dopamine D1 receptor [13]. These results also indicate decreased signaling through D2 receptor, although these could be the result of decreased signaling through other G protein-coupled receptors. The results of our preliminary RNAi, although far from conclusive, are consistent with a hypothesis based on recent observations in the mouse that there is a severe reduction of D2 signaling, resulting in relative excess of D1 signaling in DYT1 mouse models [14,15]. We will also examine the effects of neuronal RNAi expression of other neurotransmitter receptor genes, especially G-protein coupled receptors, since we have detected strong interactions between *dtorsin*-null and RNAi of three G-proteins. We will test RNAi lines for acetylcholine receptors, glutamate receptors, adenosine receptor, other G-proteins, adenylate cyclase, phospholipase-C, and other downstream signaling molecules.

(B) RNP transport pathway

We have recently demonstrated that dtorsin is required for the transport of the large RNPs from the nucleus [16]. We have tested RNAi lines of the genes (Lamin C, par6, aPKC, and baz) that had been shown to be involved in this newly discovered nuclear egress pathway [16,17]. All of the four RNAi lines for these genes (Lamin C (column 26), par6 (column 27), aPKC (column 28), and baz (column 29)) were identified as weak to moderately strong enhancers ($p<0.005$). RNAis for staufen and Fmr1, known components of RNP granules [18], are moderately strong suppressors (Table 1). These results are consistent with our hypothesis that dtorsin regulates RNP exit/transport pathway [16]. We will continue to test RNAi lines for other known genes that are involved in regulation of RNP transport including hnRNPA2, PABP (PolyA-binding protein), wg, fz2, Grip, and arm [17,18].

(C) Axon guidance and cell migration pathway

Among the strongest enhancers and suppressors are RNAis for genes that regulate axon guidance and cell migration: Fas2, robo, leak, slit, shg, and Dwnt5 (Table 1). These genes have been shown to regulate axon guidance and neuronal migration during neuronal development [19,20]. These results are consistent with a hypothesis that torsin regulates cell migration during neuronal development and torsinA mutation affects cell migration in torsinA knockout mouse models [21,22]. We will test RNAi lines for genes that are known to regulate axon guidance [19,20]. Molecular machineries for regulation of cell migration have been studied most extensively on the mechanism of primordial germ cell migration in *Drosophila* [23]. We will test RNAis for these genes as well.

(D) Other dystonia genes

Our preliminary results identified that RNAi for other dystonia genes as modifiers of *dtorsin*-null locomotion phenotype. Punch/GTPCH (an ortholog of GCH1/DYT5a) [1] (column 3) as a strong enhancer , Gαs, (an ortholog of GNAL/DYT25) [24] (column 20) as a strong suppressor , and Taf1 (an ortholog of TAF1/DYT3) [25,26] as a strong enhancer (data not shown). These results suggest a possibility that other dystonia genes, especially early-onset genes, are affecting the same signaling pathway as TOR1A/DYT1. We will test orthologs of other early onset dystonia genes including TUBB4/DYT4 [27] (three fly homologs, βTub56D, βTub60D, and βTub85D), Thap1/DYT6 [28] (two fly homologs, CG14965 and CG10431), and PRKRA/DYT16 [29] (one fly ortholog, *loqs*). We will also test RNAi line for orthologs of newly identified dystonia genes when they become known.

Once we identify candidate modifier gene, we will test second, independent RNAi line for the same gene. As an example, we have already tested three independent RNAi lines for D2R gene and all of these three were identified as strong enhancers (two of the results are shown, Fig 8 column 10 and 11). We will test the effects of neuronal RNAi expression in wild type background for strong modifiers. This will be done by crossing male RNAi lines to female elavGAL4 line (Bloomington Stock Center) and examining larval locomotion in the progeny. All of the strong enhancer RNAi lines tested so far showed no statistically significant effect on larval locomotion, suggesting the interactions we have detected for these genes are specific to dtorsin signaling pathway (data not shown).

KEY RESEARCH ACCOMPLISHMENT:

- **Establishment of UAS-human torsinAΔE and UAS-dtorsinΔE transgenic lines.**

- **Demonstration of dominant-negative activities of human torsinAΔE and dtorsinΔE proteins on larval locomotion in *Drosophila*.**

- **Demonstration of dominant-negative activities of human torsinAΔE and dtorsinΔE proteins on GTP cyclohydrolase protein levels in *Drosophila* brains. These results suggested that the same molecular pathways are regulating locomotion between human and *Drosophila.***

- **Establishment of fly lines expressing both human wild type torsinA and human torsinAΔE in *Drosophila*. These lines can be used to study the effects of human torsinAΔE mutation on locomotion in *Drosophila*. These lines will be available upon request and will be donated to public stock centers in near future.**

- **We have conducted RNAi screen to identify candidate genes that can modify *dtorsin*-null locomotion phenotypes. We are currently continuing this RNAi screen and are planning to publish our results in near future.**

•

REPORTABLE OUTCOMES:

◆Manuscripts, abstracts, presentations:

(1) Jokhi V, Ashley J, Nunnari J, Noma A, **Ito N,** Wakabayashi-Ito N, Moore MJ, and Budnik V. (2013) Torsin mediates primary envelopment of large ribonucleoprotein granules at the nuclear envelope. Cell Rep 3(4): 988-95. PMCID: PMC3683601

(2) Wakabayashi-Ito N, Ajjuri, RR, Henderson BW, Doherty OM, Breakefield XO, O'Donnell JM, and **Ito N.** (2014) Mutant human torsinA, responsible for early-onset dystonia, dominantly suppresses GTPCH expression, dopamine levels and locomotion in *Drosophila melanogaster*. PLoS One (provisionally accepted)

◆Development of fly lines:

(1) Transgenic line with human torsinAΔE302
   (a) *w-*; UAS-htorsinAΔE (II)

(2) Transgenic line with *Drosophila* dtorsinΔE306
   (a) *w-*; UAS-dtorsinΔE(#21)(III)

◆Development of DYT1 disease animal model:

(1) We have created a fly line carrying human wild type torsinA and mutant torsinA
   (a) *w-*; UAS-htorsinA(#8), UAS-htorsinAΔE(#24)(II)

(2) We have created a fly line carrying *Drosophila* wild type dtorsin and mutant dtorsin
   (a) *w-*; UAS-dtorsin(B5)(II), UAS-dtorsinΔE(#21)(III)

These fly lines are available upon request. We will deposit these fly lines to Drosophila Stock Center in near future.

◆Funding applied for based on work supported by this work:

Identification of torsin signaling pathways 04/01/14-03/31/16
NIH-NINDS R03, Ito, N. (PI)
The goal of this proposal is to identify torsin signaling pathway in *Drosophila* by conducting RNAi screen. We expect to identify genes that are in the torsin signaling pathways by examining the effects of RNAi expression in Drosophila neurons in *dtorsin*-null flies. (Not funded).

Pathway discovery for early-onset gene DYT1 1/01/14-12/31/14
Bachmann-Strauss Dystonia & Parkinson Foundation
Ito (PI)
The goal of this project is to study the function of the *Drosophila dtorsin* gene using the *dtorsin* null mutants by conducting RNAi screen. (Not funded).

Pathway discovery for early-onset dystonia gene 07/01/14-06/30/16
DOD, Peer Reviewed Medical Research Program
Ito (PI)
The goal of this proposal is to identify torsin signaling pathway in *Drosophila* by conducting RNAi screen. We expect to identify genes that are in the torsin signaling pathways by examining the effects

of RNAi expression in *Drosophila* neurons in *dtorsin*-null flies focusing on neurotransmitter signaling, RNP transport, and axon guidance pathways. (Not funded).

CONCLUSION:

(1) We have created fly lines expressing human torsinAΔE in their brains. The phenotypes caused by the expression of human torsinAΔE in the fly brains were indistinguishable from those caused by *dtorsin*-null mutation (reduced locomotion and reduced GTPCH protein levels). These results suggested that underlying molecular defects caused by human torsinA mutation can be studied in our fly system.

(2) By using RNAi fly lines available from the fly stock centers and expressing RNAi molecules in *dtorsin*-null fly brains, we can quickly indentify genes whose mutation can modify the *dtorsin*-null locomotion phenotypes. Our fly system will be very useful for identifying torsin signal transduction pathways. We have already identified: (1) dopamine synthesis pathway, (2) dopamine receptor signaling pathway, (3) RNP transport pathway, and (4) axon guidance pathway as modifiers of torsin signaling pathway. Identification of these pathways will allow us to identify potential therapeutic targets for not only for DYT1 patients, but also for other dystonia patients. We have also identified potential genetic interactions between different dystonia genes. We are continuing our efforts to identify torsin signaling pathways. These preliminary studies already gave us deeper insights into the defects caused by the *dtorsin* mutations.

REFERENCES:

1. Wakabayashi-Ito N, Doherty OM, Moriyama H, Breakefield XO, Gusella JF, et al. (2011) dtorsin, the Drosophila Ortholog of the Early-Onset Dystonia TOR1A (DYT1), Plays a Novel Role in Dopamine Metabolism. PLoS One 6: e26183.
2. Brand AH, Perrimon N (1993) Targeted gene expression as a means of altering cell fates and generating dominant phenotypes. Development 118: 401-415.
3. Hewett J, Gonzalez-Agosti C, Slater D, Ziefer P, Li S, et al. (2000) Mutant torsinA, responsible for early-onset torsion dystonia, forms membrane inclusions in cultured neural cells. Hum Mol Genet 9: 1403-1413.
4. Song W, Onishi M, Jan LY, Jan YN (2007) Peripheral multidendritic sensory neurons are necessary for rhythmic locomotion behavior in Drosophila larvae. Proc Natl Acad Sci U S A 104: 5199-5204.
5. Bragg DC, Camp SM, Kaufman CA, Wilbur JD, Boston H, et al. (2004) Perinuclear biogenesis of mutant torsin-A inclusions in cultured cells infected with tetracycline-regulated herpes simplex virus type 1 amplicon vectors. Neuroscience 125: 651-661.
6. Chaudhuri A, Bowling K, Funderburk C, Lawal H, Inamdar A, et al. (2007) Interaction of genetic and environmental factors in a Drosophila parkinsonism model. Journal of Neuroscience 27: 2457-2467.
7. Ni JQ, Liu LP, Binari R, Hardy R, Shim HS, et al. (2009) A Drosophila resource of transgenic RNAi lines for neurogenetics. Genetics 182: 1089-1100.
8. Ni JQ, Zhou R, Czech B, Liu LP, Holderbaum L, et al. (2011) A genome-scale shRNA resource for transgenic RNAi in Drosophila. Nat Methods 8: 405-407.
9. Dietzl G, Chen D, Schnorrer F, Su KC, Barinova Y, et al. (2007) A genome-wide transgenic RNAi library for conditional gene inactivation in Drosophila. Nature 448: 151-156.
10. van der Bliek AM, Meyerowitz EM (1991) Dynamin-like protein encoded by the Drosophila shibire gene associated with vesicular traffic. Nature 351: 411-414.
11. Vallee RB, Herskovits JS, Aghajanian JG, Burgess CC, Shpetner HS (1993) Dynamin, a GTPase involved in the initial stages of endocytosis. Ciba Found Symp 176: 185-193; discussion 193-187.
12. Kume K, Kume S, Park SK, Hirsh J, Jackson FR (2005) Dopamine is a regulator of arousal in the fruit fly. J Neurosci 25: 7377-7384.
13. Tritsch NX, Sabatini BL (2012) Dopaminergic modulation of synaptic transmission in cortex and striatum. Neuron 76: 33-50.
14. Sciamanna G, Bonsi P, Tassone A, Cuomo D, Tscherter A, et al. (2009) Impaired striatal D2 receptor function leads to enhanced GABA transmission in a mouse model of DYT1 dystonia. Neurobiol Dis 34: 133-145.
15. Sciamanna G, Tassone A, Mandolesi G, Puglisi F, Ponterio G, et al. (2012) Cholinergic Dysfunction Alters Synaptic Integration between Thalamostriatal and Corticostriatal Inputs in DYT1 Dystonia. J Neurosci 32: 11991-12004.
16. Jokhi V, Ashley J, Nunnari J, Noma A, Ito N, et al. (2013) Torsin mediates primary envelopment of large ribonucleoprotein granules at the nuclear envelope. Cell Rep 3: 988-995.
17. Speese SD, Ashley J, Jokhi V, Nunnari J, Barria R, et al. (2012) Nuclear envelope budding enables large ribonucleoprotein particle export during synaptic Wnt signaling. Cell 149: 832-846.
18. Kiebler MA, Bassell GJ (2006) Neuronal RNA granules: movers and makers. Neuron 51: 685-690.
19. Araujo SJ, Tear G (2003) Axon guidance mechanisms and molecules: lessons from invertebrates. Nat Rev Neurosci 4: 910-922.
20. Kolodkin AL, Tessier-Lavigne M (2011) Mechanisms and molecules of neuronal wiring: a primer. Cold Spring Harb Perspect Biol 3.
21. Nery FC, Zeng J, Niland BP, Hewett J, Farley J, et al. (2008) TorsinA binds the KASH domain of nesprins and participates in linkage between nuclear envelope and cytoskeleton. J Cell Sci 121: 3476-3486.

22. McCarthy DM, Gioioso V, Zhang X, Sharma N, Bhide PG (2012) Neurogenesis and neuronal migration in the forebrain of the TorsinA knockout mouse embryo. Dev Neurosci 34: 366-378.
23. Richardson BE, Lehmann R (2010) Mechanisms guiding primordial germ cell migration: strategies from different organisms. Nat Rev Mol Cell Biol 11: 37-49.
24. Fuchs T, Saunders-Pullman R, Masuho I, Luciano MS, Raymond D, et al. (2013) Mutations in GNAL cause primary torsion dystonia. Nat Genet 45: 88-92.
25. Makino S, Kaji R, Ando S, Tomizawa M, Yasuno K, et al. (2007) Reduced neuron-specific expression of the TAF1 gene is associated with X-linked dystonia-parkinsonism. Am J Hum Genet 80: 393-406.
26. Herzfeld T, Nolte D, Grznarova M, Hofmann A, Schultze JL, et al. (2013) X-linked dystonia parkinsonism syndrome (XDP, lubag): disease-specific sequence change DSC3 in TAF1/DYT3 affects genes in vesicular transport and dopamine metabolism. Hum Mol Genet 22: 941-951.
27. Lohmann K, Wilcox RA, Winkler S, Ramirez A, Rakovic A, et al. (2012) Whispering dysphonia (DYT4 dystonia) is caused by a mutation in the TUBB4 gene. Ann Neurol.
28. Bragg DC, Armata IA, Nery FC, Breakefield XO, Sharma N (2011) Molecular pathways in dystonia. Neurobiol Dis 42: 136-147.
29. Camargos S, Scholz S, Simon-Sanchez J, Paisan-Ruiz C, Lewis P, et al. (2008) DYT16, a novel young-onset dystonia-parkinsonism disorder: identification of a segregating mutation in the stress-response protein PRKRA. Lancet Neurol 7: 207-215.

Cell PRESS
Open ACCESS

Cell Reports
Report

Torsin Mediates Primary Envelopment of Large Ribonucleoprotein Granules at the Nuclear Envelope

Vahbiz Jokhi,[1,4] James Ashley,[1,4] John Nunnari,[1] Akiko Noma,[2] Naoto Ito,[3] Noriko Wakabayashi-Ito,[3] Melissa J. Moore,[2] and Vivian Budnik[1,*]

[1]Department of Neurobiology
[2]RNA and Neuro Therapeutics Institutes, Department of Biochemistry and Molecular Pharmacology, Howard Hughes Medical Institute University of Massachusetts Medical School, Worcester, MA 01605, USA
[3]Department of Neurology and Radiology, Massachusetts General Hospital and Program in Neuroscience, Harvard Medical School, Boston, MA 02114, USA
[4]These authors contributed equally to this work
*Correspondence: vivian.budnik@umassmed.edu
http://dx.doi.org/10.1016/j.celrep.2013.03.015

SUMMARY

A previously unrecognized mechanism through which large ribonucleoprotein (megaRNP) granules exit the nucleus is by budding through the nuclear envelope (NE). This mechanism is akin to the nuclear egress of herpes-type viruses and is essential for proper synapse development. However, the molecular machinery required to remodel the NE during this process is unknown. Here, we identify Torsin, an AAA-ATPase that in humans is linked to dystonia, as a major mediator of primary megaRNP envelopment during NE budding. In *torsin* mutants, megaRNPs accumulate within the perinuclear space, and the messenger RNAs contained within fail to reach synaptic sites, preventing normal synaptic protein synthesis and thus proper synaptic bouton development. These studies begin to establish the cellular machinery underlying the exit of megaRNPs via budding, offer an explanation for the "nuclear blebbing" phenotype found in dystonia models, and provide an important link between Torsin and the synaptic phenotypes observed in dystonia.

INTRODUCTION

Polarized assembly of cellular complexes often depends on formation of translationally silent RNA transport granules containing mRNAs and associated structural and regulatory components (e.g., proteins and microRNAs). These RNA-protein complexes (RNPs) are shuttled to distinct cellular locales where, upon specific stimuli, the messenger RNAs (mRNAs) are translated into protein building blocks for local cellular architectures and macromolecular complexes (Richter, 2001). Particularly notable is RNP transport in the nervous system, where long-term changes in synaptic structure and function frame key events enabling organisms to respond to their changing environment. A special case of this adaptation is the ability of organisms to learn and remember (Wiersma-Meems et al., 2005). In these processes, localized translation of mRNAs links synaptic-plasticity-inducing stimuli to the synthesis of effector proteins underlying enduring changes in synaptic structure and function (Barco et al., 2008).

Until recently, it was thought that all mRNA export occurred one molecule at a time through the nuclear pore complex (NPC) (Grünwald et al., 2011; Köhler and Hurt, 2007). However, we recently uncovered a mechanism by which large ribonucleoprotein (megaRNP) granules exit the nucleus via nuclear envelope (NE) budding (Speese et al., 2012), a mechanism previously shown to be utilized for the nuclear export of large herpes-type viral capsids (Maric et al., 2011; Mettenleiter et al., 2006). This budding process and the signaling pathway that it initiates are essential for normal synaptic bouton development at the *Drosophila* larval neuromuscular junction (NMJ) (Ataman et al., 2006; Mathew et al., 2005; Speese et al., 2012). NE budding entails primary envelopment of viral capsids (Mettenleiter et al., 2006) or megaRNPs (Speese et al., 2012) by the inner nuclear membrane (INM); scission of this envelope from the INM creates a membrane-bound particle within the perinuclear space, which subsequently fuses with the outer nuclear membrane (ONM) to allow nuclear escape of the enclosed material. However, the molecular mechanisms required for primary envelopment, INM scission, and fusion were previously unknown. Here, we identify Torsin, an AAA-ATPase that in humans is linked to both dystonia (Breakefield et al., 2008) and herpes virus nuclear egress (Maric et al., 2011), as a major mediator of primary megaRNP envelopment during NE budding, likely functioning to promote INM scission. In *torsin* mutants, including those mimicking genetic abnormalities in dystonia patients, megaRNPs accumulate within the perinuclear space and the mRNAs contained within fail to reach synaptic sites, preventing normal synaptic protein synthesis and thus proper synaptic bouton development.

RESULTS AND DISCUSSION

In humans, the dystonia-specific *Torsin1A* (*TOR1A*) mutation $TOR1A^{\Delta E302/303}$ (also known as $TOR1A^{\Delta GAG}$; referred to as $Torsin^{\Delta E}$ in this paper) at the DYT1 gene locus is linked to

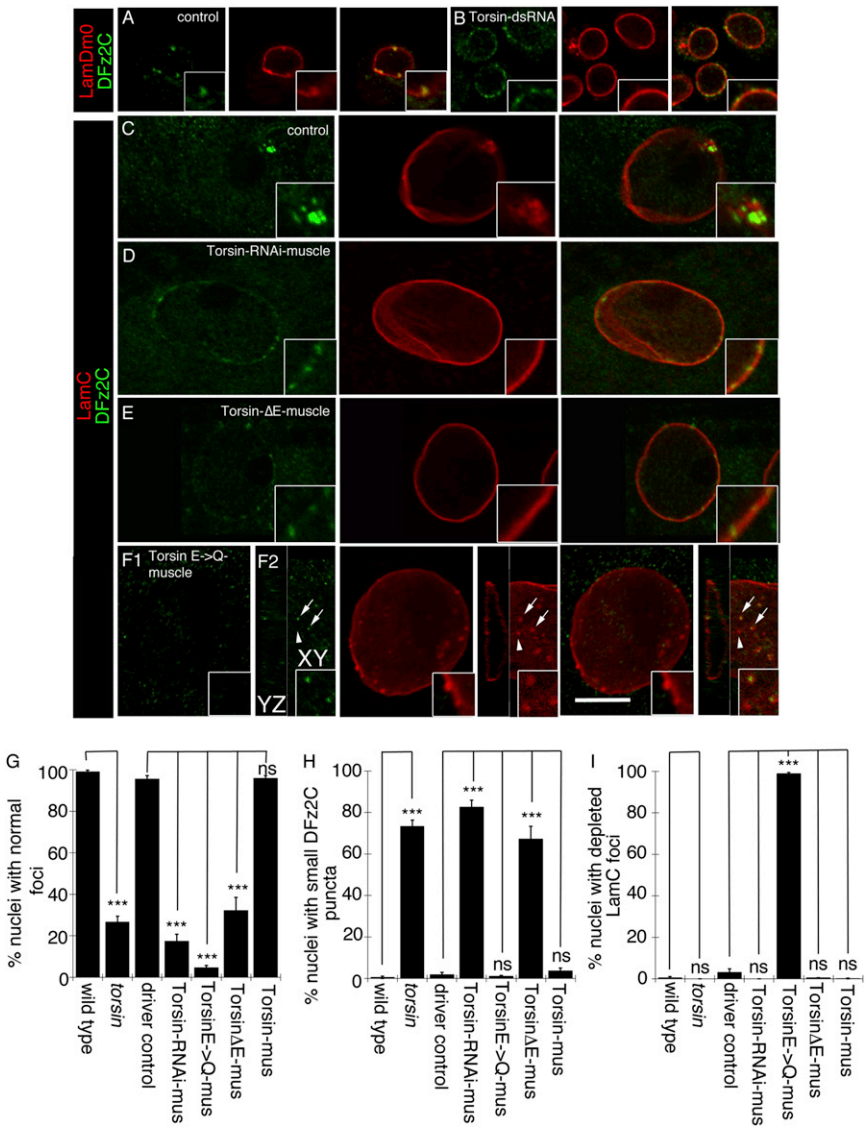

Figure 1. Morphology of Nuclear DFz2C/Lam Foci Is Disrupted in Torsin Mutations

(A and B) Localization and morphology of DFz2C/Lam foci at the nuclei of S2 cells in (A) untreated cells and (B) cells treated with Torsin-dsRNA.

(C–F) Localization and morphology of nuclear DFz2C/LamC foci in larval muscles of (C) wild-type and (D–F) larvae expressing (D) Torsin RNAi, (E) Torsin$^{\Delta E}$, and (F) Torsin$^{E\rightarrow Q}$ in muscles. F1 is a low-magnification view. F2 shows a high-magnification view of DFz2 puncta in the YZ and XY planes. (A)–(F) correspond to singe confocal slices.

(G–I) Percentage of nuclear foci showing (G) normal organization of DFz2C/LamC, (H) the presence of small DFz2C puncta associated with the lamina (see text), and (I) the presence of thickenings of the lamina devoid of DFz2C signal. Mus, muscle; N([number of nuclei;number of larvae]), [908;6],[731;6],[639;6],[802;6],[846;6],[733;6],[693;6]. Error bars represent ±SEM; ***$p < 0.0001$.

Calibration scales are 14 μm (4 μm for insets) in (A) and (B) and 10 μm (6 μm for insets) in (C)–(F). See also Figure S1.

early-onset primary dystonia (Tanabe et al., 2009). Mouse models expressing *TOR1A*$^{\Delta E302/303}$ accumulate abnormal vesicular structures at the NE (Goodchild et al., 2005; Naismith et al., 2004). These NE structures show a striking resemblance to the perinuclear megaRNPs we recently reported in *Drosophila* (Speese et al., 2012), raising the intriguing possibility that these structures could be related. In cultured Schneider-2 (S2) cells and *Drosophila* larval muscles, megaRNP clusters at the NE can be marked at the light microscopy level by antibodies to the C terminus of the Wnt receptor DFrizzled2 (DFz2C) and the INM-associated protein Lamin C (LamC). DFz2C and LamC partially colocalize at NE-associated foci (DFz2C/LamC foci) (Mathew et al., 2005; Speese et al., 2012). To determine if NE defects observed in *TOR1A* mutant animal models reflect defects in NE budding, S2 cells were treated with Torsin double-stranded RNA (dsRNA), targeting the sole *Drosophila* homolog of mammalian *TOR1A* (Wakabayashi-Ito et al., 2011) (see Figure S1 for Torsin-dsRNA efficiency). This resulted in significant abnormalities in DFz2C/LamC foci at the NE. In untreated S2 cells, NE-DFz2C foci appear as bright immunoreactive spots embedded in a thickening of the lamina, marked by LamC (Speese et al., 2012) or the B-type lamin LamDm0 (Figure 1A). In contrast, Torsin-dsRNA-treated cells displayed small DFz2C-immunoreactive puncta dotting the NE, and thickenings of the lamina were barely visible or absent (Figure 1B; see below for quantification of this phenotype in vivo).

In mammals, Torsin isoforms are derived from four genes: *Tor1A*, *Tor1B*, *Tor2A*, and *Tor3A*. The DYT1 mutation in *Tor1A* specifically affects the neuronal NE (Goodchild et al., 2005), consistent with the belief that dystonia is a disease of the nervous system. This neuronal specificity is likely due to compensation by expression of torsinB in nonneuronal tissues, as knockdown of TOR1B in a DYT mutant background caused NE defects in nonneuronal cells (Kim et al., 2010). In *Drosophila*, there is a single *torsin* gene, thus overcoming difficulties associated with redundancy. Moreover, we previously showed that NE budding occurs in several cell types, including larval body wall muscle cells wherein the large nuclei are particularly suitable for high-resolution studies (Speese et al., 2012). In addition, the glutamatergic larval NMJ is a powerful model system in which to understand mechanisms of synapse development and function.

To determine the significance of the S2 cell NE phenotype upon Torsin downregulation, DFz2C/LamC foci were examined in *torsin*^{KO78}-null mutants (Wakabayashi-Ito et al., 2011) and in

larvae in which Torsin was specifically downregulated in muscles by expressing Torsin RNAi using the muscle-specific Gal4 driver C57-Gal4 (Budnik et al., 1996). As in untreated S2 cells, NE DFz2C/LamC foci were observed in wild-type larvae as DFz2C immunoreactive spots surrounded by a thickening of LamC immunoreactivity (Speese et al., 2012) (Figure 1C). In contrast, in larvae expressing Torsin-RNAi in muscles (Figure 1D) or in *torsin*-null mutants, DFz2C foci were observed as small puncta decorating the NE but lacking any detectable thickening of the lamina. These phenotypes were quantified by determining the percentage of nuclei containing DFz2C spots surrounded by a thickening of the lamina (normal foci; Figure 1G) and the percentage of nuclei containing small NE-associated DFz2C puncta lacking LamC thickening (Figure 1H). There were highly significant differences between wild-type controls and both *torsin*-null mutants as well as larvae expressing Torsin-RNAi in muscles (Figures 1G and 1H).

Typical of AAA-ATPases, Torsin contains Walker A and Walker B domains involved in ATP binding and ATP hydrolysis, respectively (Neuwald et al., 1999; Wakabayashi-Ito et al., 2011; Walker et al., 1982), as well as Sensor1 and Sensor2 domains also involved in ATP hydrolysis (Iyer et al., 2004). A conserved amino acid deletion in the Sensor2 domain (Torsin$^{\Delta E}$; Torsin$^{\Delta E306}$ in *Drosophila*) is dominantly linked to dystonia (Ozelius et al., 1997). In addition, an amino acid substitution in the Walker B domain (Torsin$^{E\rightarrow Q}$; Torsin^{E177Q} in *Drosophila*) leads to a Torsin protein that can dominantly bind to its substrate but is unable to hydrolyze ATP and therefore remains bound to this substrate, thus constituting a substrate trap (Goodchild et al., 2005; Wakabayashi-Ito et al., 2011). To determine if Torsin$^{\Delta E}$ or Torsin$^{E\rightarrow Q}$ transgene expression would also disrupt DFz2C/LamC foci morphology, we expressed these proteins in larval muscles. Expressing Torsin$^{\Delta E}$ mimicked the *torsin*-null and Torsin-RNAi phenotypes (Figures 1E, 1G, and 1H). In contrast, Torsin$^{E\rightarrow Q}$ expression resulted in the formation of numerous NE LamC foci, most of which were devoid of DFz2C immunoreactivity (Figures 1F1 and 1G–1I). Careful examination of these depleted LamC foci by confocal microscopy demonstrated that many contained a small DFz2C puncta, but this signal was barely visible (Figure 1F2, arrows). The above phenotypes observed upon expressing Torsin$^{\Delta E}$ and Torsin$^{E\rightarrow Q}$ were the specific results of the mutations in the Torsin transgenes, as larvae expressing a wild-type Torsin transgene were indistinguishable from wild-type not expressing this transgene (Figures 1G–1I).

To determine the ultrastructural correlates of the above phenotypes, untreated and Torsin-dsRNA-treated S2 cells were examined by transmission electron microscopy (TEM). As previously described (Speese et al., 2012), untreated S2 cells displayed local singlets or clusters of megaRNPs within INM invaginations at discrete regions of the NE (Figures 2A, 2H, and 2I), paralleling light microscopy observations (Figure 1A). In contrast, in Torsin-dsRNA-treated cells, these local megaRNPs at the NE were reduced by ~75% (Figures 2H and 2I), and instead many mega-RNP granules were often observed in rows of singlets lining the perinuclear space (Figures 2B and 2C). In these regions, the perinuclear space appeared distended (green in Figures 2B and 2C) and the ribosome-decorated ONM appeared to evaginate (Figures 2B and 2C). However, NPCs and the rest of the NE appeared normal (Figures S2A–S2D). In addition, the distribution of a number of nuclear proteins, such as the fly Emerin homolog Bocksbeutel (Figures S2E and S2I); dMan1 (Figures S2F and S2J); Otefin, a protein required for NE assembly (Figures S2G and S2K); and the *Drosophila* homolog of Hsap, Squid, a ribonuclear protein (Figures S2H and S2L), were normally distributed in the mutants. About half of megaRNPs appeared attached to the INM through a collared neck (arrows in Figures 2B, 2C, 2H, and 2I; see Experimental Procedures for definition). Thus, downregulating Torsin results in abnormal attachment of megaRNPs to the INM, raising the possibility that Torsin could be involved in INM scission after primary megaRNP envelopment.

Corroboration of the above results in vivo was obtained by examining larval body wall muscles of *torsin*-null mutants. As in S2 cells, megaRNPs tethered to the INM by a collared neck were observed in *torsin*-null mutant muscles and epithelial cells (Figures 2D, 2E, 2H, and 2I), suggesting this pathway functions in even more tissues than previously characterized. Similarly, muscles expressing Torsin$^{E\rightarrow Q}$ displayed INM-tethered megaRNPs (Figures 2F, 2H, and 2I). In ~30% of cases, megaRNPs in muscles expressing Torsin$^{E\rightarrow Q}$ appeared as large (>250 nm), amorphous, dense structures directly apposed to the INM (Figures 2G–2I). Thus, disruption of Torsin function in vivo leads to abnormal megaRNP tethering to the INM.

If Torsin is involved in INM scission during megaRNP primary envelopment, then the substrate trap Torsin$^{E\rightarrow Q}$ should accumulate at the electron-dense collared necks. This prediction was tested by generating wild-type and Torsin$^{E\rightarrow Q}$ variants fused to a mini-SOG tag (Shu et al., 2011) at their C termini. Mini-SOG is a flavoprotein derived from *Arabidopsis* Phototropin 2 that when illuminated by blue light produces oxygen species that can convert diaminobenzidine into an electron-dense precipitate (Shu et al., 2011).

We first determined if C-terminally tagged Torsin was localized to the NE. Although mini-SOG excitation results in fluorescence emission, its rapid bleaching upon illumination prevented high-resolution acquisition of images. Therefore, we generated Flag-tagged Torsin constructs and expressed them in S2 cells. The wild-type Torsin-Flag signal localized to bright spots coinciding with Lamin foci at the NE; low levels were also observed at the NE and in the cytoplasm (Figure 3A). In contrast, Torsin$^{E\rightarrow Q}$-Flag was observed in a punctate pattern lining the NE (Figure 3B).

Consistent with the above observations, S2 cells expressing Torsin-SOG displayed an electron-dense signal at sites of megaRNP occurrence in the NE (Figures 3C and 3E; see Figures S3A and S3B for specificity control). An electron-dense SOG-induced signal surrounded each megaRNP (Figures 3C and 3E) in a relatively homogenous fashion, but local accumulations of the signal were also apparent (arrows in Figure 3E). A SOG-specific signal was also observed at the INM and ONM in proximity to megaRNPs (Figure 3E). In contrast, in cells expressing the substrate trap Torsin$^{E\rightarrow Q}$-SOG, a SOG-induced signal was concentrated at collared necks of INM-associated megaRNPs and little SOG signal surrounded the megaRNPs (Figures 3D and 3F). In cases where large amorphous megaRNPs were tightly apposed to the INM in Torsin$^{E\rightarrow Q}$, the SOG signal was considerably denser at the sites of contact between the megaRNP and the INM (Figure 3G). These observations suggest

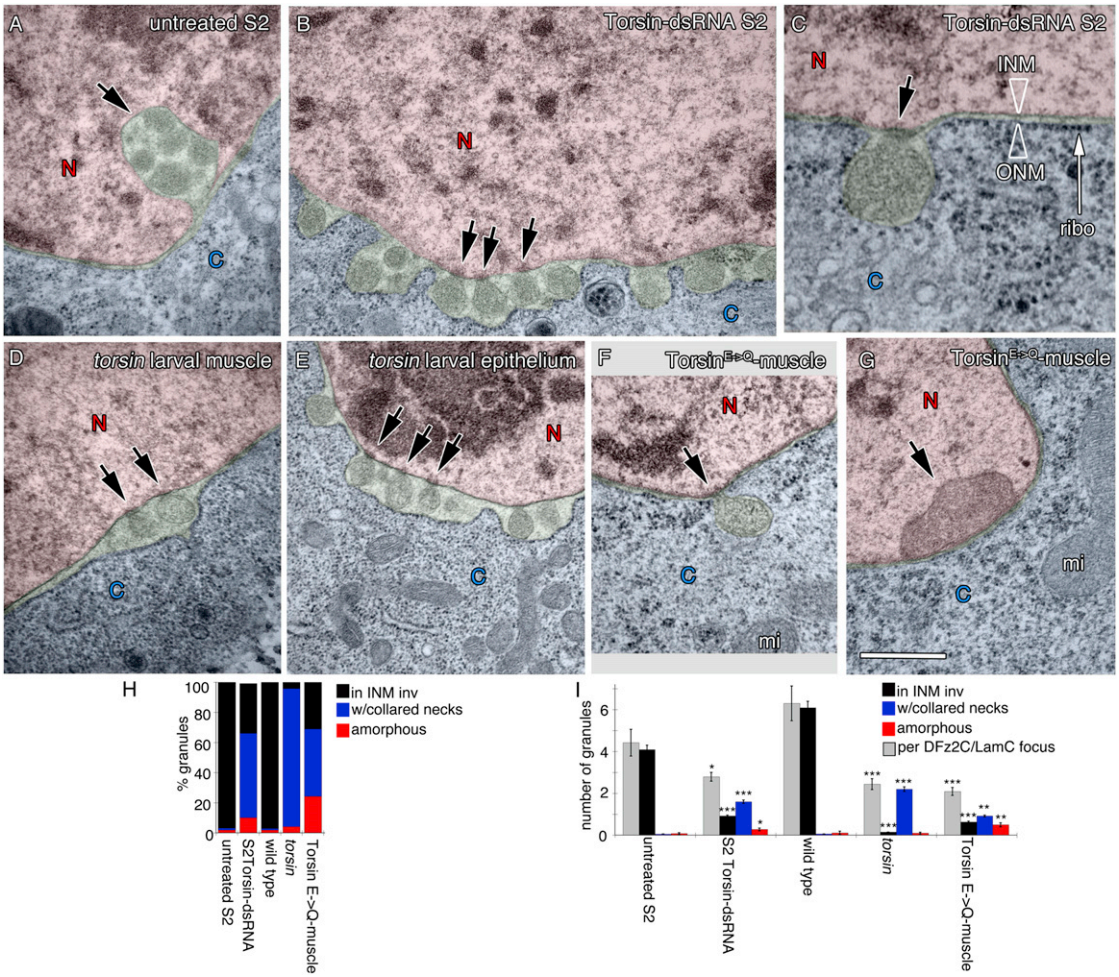

Figure 2. Ultrastructural Organization of NE-Associated megaRNPs Is Disrupted in Torsin Mutations

(A–G) Electron micrographs of nuclear regions in (A–C) S2 cells, (D, F, and G) larval body wall muscles, and (E) larval epithelial cells showing NE-associated megaRNPs. Red, nucleus; blue, cytoplasm; green, perinuclear space. N, nucleus; C, cytoplasm. (A) Untreated S2 cell showing a normal nuclear focus (arrow) containing electron-dense megaRNP granules. (B and C) NE of Torsin-dsRNA-treated S2 cells displaying megaRNPs tethered to the INM by collared necks (arrows), shown at (B) low and (C) high magnification. ribo, ribosome. (D and E) NE in *torsin*-null mutants also showing megaRNPs tethered to the INM (arrows). (F and G) NE in muscle cells expressing Torsin$^{E\to Q}$ showing the presence of (F) a megaRNP (arrow) tethered to the INM and (G) a large, amorphous megaRNP (arrow) tightly apposed to the INM. mi, mitochondria.

(H) Percentage of megaRNP granules present in INM invaginations (black), with collared necks (blue) and being large and amorphous (red).

(I) Average number of megaRNP granules in INM invaginations (black), with collared necks (blue), being large and amorphous (red), or per focus (gray). N[number of granules;foci]), [159;36],[366;122],[207;33],[166;68],[181;88]. Error bars represent ±SEM; *$p < 0.05$; **$p < 0.001$; ***$p < 0.0001$).

Calibration scales are 0.5 μm (A, B, and D–G) and 0.2 μm (C). See also Figure S2.

that Torsin is present at sites of NE budding. Further, accumulation of the Torsin$^{E\to Q}$ substrate trap protein at collared necks of megaRNPs suggests that these necks represent the normal site of Torsin action and provide evidence that Torsin is involved in scission of the INM during primary envelopment.

Our previous study revealed that in *Drosophila* larval muscles, megaRNPs contain transcripts encoding postsynaptic proteins, including the PDZ scaffolding proteins Par6 and MAGI (Speese et al., 2012). In the case of Par6, interfering with megaRNP formation by inhibiting the Frizzled nuclear import (FNI) pathway or LamC expression results in decreased NMJ localization of *par6* mRNA (Speese et al., 2012), decreased postsynaptic Par6 protein levels (Speese et al., 2012), and marked defects in NMJ structure (Ataman et al., 2006, 2008; Packard et al., 2002; Speese et al., 2012). In particular, under these conditions, NMJs fail to expand normally as muscles grow in size during larval development, and a subset of synaptic boutons (called ghost boutons) remain in an immature state. These ghost boutons fail to recruit postsynaptic proteins and to organize postsynaptic specializations, such as the postsynaptic density and subsynaptic reticulum (Ataman et al., 2006, 2008; Packard et al., 2002; Speese et al., 2012).

The above observations support a model in which alterations in Torsin function inhibit nuclear megaRNP exit by slowing or

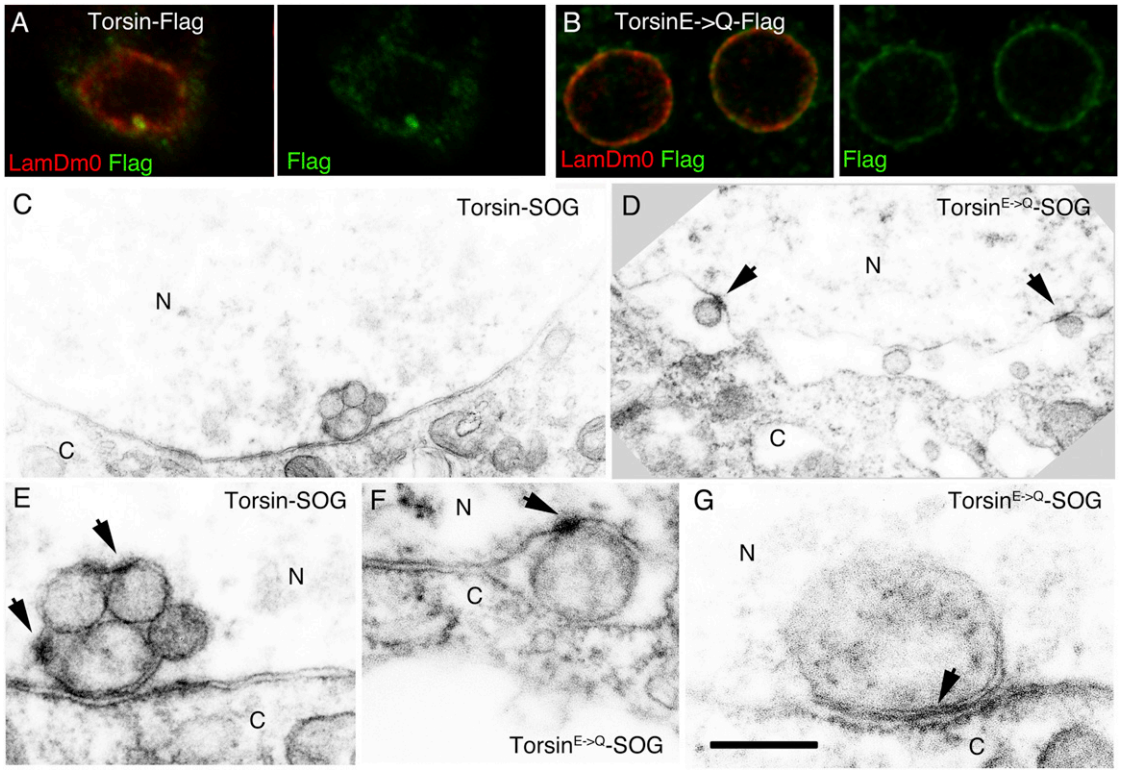

Figure 3. The Torsin$^{E\rightarrow Q}$ Protein Accumulates at megaRNP Collared Necks

(A and B) S2 cells expressing (A) wild-type Torsin-Flag and (B) the Torsin$^{E\rightarrow Q}$-Flag showing that Torsin-Flag accumulates at foci and Torsin$^{E\rightarrow Q}$ is punctate at the NE.

(C–G) Electron micrographs of nuclear regions of S2 cells expressing (C and E) Torsin-SOG showing an electron-dense signal surrounding megaRNPs (arrows point to areas of increased signal density). (D, F, and G) Torsin$^{E\rightarrow Q}$-SOG showing that signal accumulates (D and F) at megaRNP collared necks or (G) at appositions of amorphous megaRNPs with the INM.

Calibration scales are 7 μm (A and B), 0.7 μm (C and D), and 0.3 μm (E–G). See also Figure S3.

blocking INM scission during primary envelopment. As a consequence, such alterations should result in abnormal transcript localization both in the nucleus and at synaptic sites as well as decreased synaptic protein synthesis, abnormal NMJ expansion, and an accumulation of ghost boutons. To ascertain the localization of megaRNP transcripts known to be present in megaRNPs at the NE, we carried out fluorescence in situ hybridization (FISH) using *par6* and *magi* RNA probes. As previously described (Speese et al., 2012), in wild-type muscles, *par6* and *magi* mRNAs are enriched at NE foci associated with LamC foci or nuclear folds marked by antibodies to LamC (Figures 4A and 4B, top row). In contrast, in *torsin*-null mutants, *par6* and *magi* FISH signals appeared as foci that, while associated with the NE, were on the cytoplasmic side of the LamC signal (Figures 4A and 4B, bottom row panels; Figure 4C). This is in agreement with the light and electron microscopy studies, showing that altering Torsin function prevents megaRNP nuclear egress and results in megaRNPs remaining attached to the INM within the perinuclear space.

When we examined FISH signals at the NMJ in wild-type controls, *par6* mRNA was concentrated at subsynaptic sites as previously reported (Figure 4D, top panels) (Speese et al., 2012). However, this synaptic *par6* FISH signal was virtually eliminated in *torsin*-null mutants (Figure 4D, bottom panels). Similarly, the synaptic localization of *magi* mRNA was significantly decreased in the *torsin* mutants (Figure 4E). The marked decrease in *par6* and *magi* mRNA levels at the NMJ appeared specific for the NE-budding pathway, as no significant differences around the NMJ in *torsin* mutants were observed upon FISH of *discs-large* (*dlg*) RNA, which is not associated with nuclear DFz2C/LamC foci (Figures S4A–S4C) (Speese et al., 2012). Thus, in the absence of Torsin function, synaptic mRNAs known to be present in megaRNPs exhibit reduced localization at the NMJ, but a nonmegaRNP mRNA does not.

We also examined Par6 and MAGI protein levels using antibodies specific to *Drosophila* Par6 (Ruiz-Canada et al., 2004) and MAGI (this report). In wild-type larvae, Par6 and MAGI immunoreactivity localized primarily to the postsynaptic muscle region of the NMJ (Figures 4F and 4G, top panels). In addition, Par6 immunoreactivity was observed in a diffuse manner at presynaptic boutons (marked by the anti-HRP signal), being particularly prominent at presynaptic microtubule bundles (Ruiz-Canada et al., 2004) (Figure 4F, top panels) and at low levels at the muscle cell cortex (Figure 4F, top panels). MAGI immunoreactivity was also observed at presynaptic compartments, but without noticeable concentration at microtubule bundles (Figure 4G, top

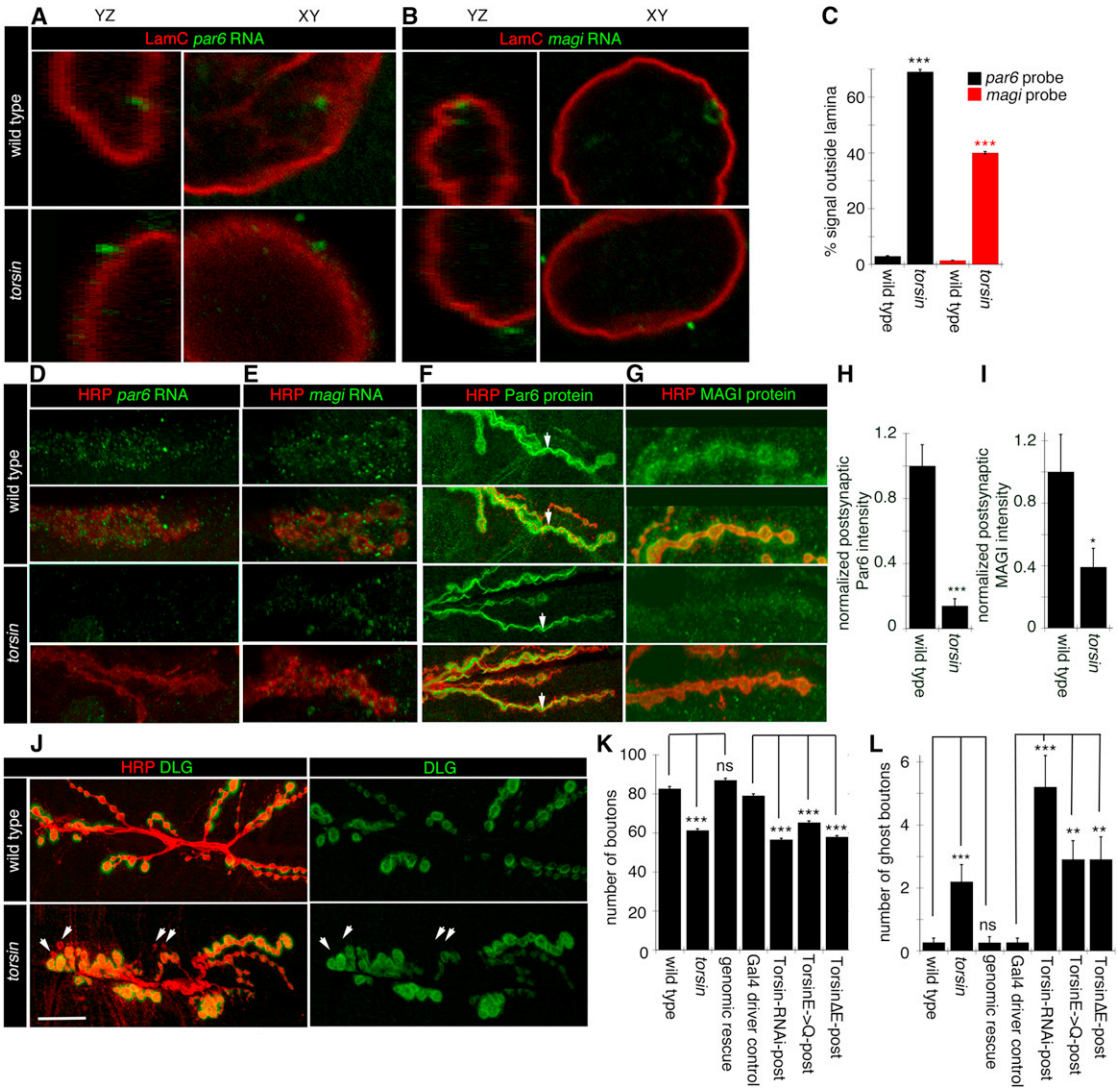

Figure 4. The Distribution of mRNAs at the NE and Synaptic Sites Is Disrupted in *torsin* Mutants

(A and B) FISH to body wall muscles showing the nuclear distribution of (A) *par6* and (B) *magi* transcripts in wild-type and *torsin* mutants.

(C) Quantification of FISH signal outside the nucleus. N [nuclei;larvae], [18;6],[18;6],[18;6],[14;6].

(D and E) FISH to body wall muscles showing the distribution of (D) *par6* and (E) *magi* transcript at the NMJ in wild-type and *torsin*-null mutants.

(F and G) Distribution of (F) Par6 and (G) Magi immunoreactivity at the NMJ in wild-type and *torsin* mutants.

(H and I) Quantification of postsynaptic (H) Par6 and (I) Magi immunoreactive signal, normalized to wild-type control. N([NMJs;larvae]) is [16;6],[18;6] (H) and [17;6],[15;6] (I).

(J) NMJs in wild-type and *torsin* mutants labeled with anti-HRP and anti-DLG showing reduced size and increased ghost boutons (arrowheads) in *torsin* mutants.

(K and L) Quantification of the number of (K) synaptic boutons and (L) ghost boutons. N([NMJs;larvae]), [19;10],[18;10],[19;10],[19;10],[20;10],[19;10],[19;10] for (K) and (L). Error bars represent ±SEM; **$p < 0.001$; ***$p < 0.0001$.

Calibration scale are 3 μm (A and B), 10 μm (D–G), and 20 μm (J). See also Figure S4.

panels). In *torsin*-null mutants, postsynaptic localization of Par6 immunoreactivity as well as muscle cell cortex signal was severely reduced (Figure 4F, bottom panels; Figure 4H), while presynaptic localization of Par6 at microtubule bundles appeared normal (Figure 4F, arrows). Similarly, postsynaptic MAGI protein localization was severely reduced in these mutants (Figure 4G, bottom panels; Figure 4I). Unlike Par6 and MAGI, DLG immunoreactivity was not changed in *torsin* mutants (Figure 4J; Figure S4D), suggesting that the defect is not general but affects only a subset of postsynaptic proteins. Thus, disrupting Torsin function prevents normal localization of some synaptic mRNAs and, as a consequence, normal postsynaptic levels of their encoded proteins.

The functional consequence on NMJ structure of reduced Par6 and MAGI mRNA and protein levels at the postsynaptic compartment in *torsin* mutants was assessed by counting the

number of normal and undifferentiated ghost boutons observable in the last (third-instar) larval stage. Interfering with Torsin function resulted in a significantly reduced number of synaptic boutons (Figures 4J and 4K) and a significantly increased number of undifferentiated ghost boutons (Figure 4J, arrowheads; Figure 4L).

Together, these results demonstrate that inhibiting Torsin function results in megaRNP accumulation at the NE, likely due to a defect in INM scission during primary envelopment. As a consequence, synaptic transcript-containing megaRNPs fail to efficiently exit the nucleus, limiting trafficking of the mRNAs contained within to postsynaptic sites where they are normally enriched. This reduced synaptic mRNA localization results in reduced levels of specific postsynaptic proteins during NMJ expansion and thus in poorly developed NMJs containing fewer synaptic boutons and increased numbers of undifferentiated ghost boutons lacking postsynaptic proteins. These results provide mechanistic insight into the molecular machinery underlying nuclear egress of megaRNPs by NE budding. They also provide a mechanism by which Torsin influences synaptic development as well as important clues as to how torsinA dysfunction might lead to the alterations in synaptic plasticity observed in DYT1 mouse models and human patients.

EXPERIMENTAL PROCEDURES

Fly Strains

Flies were reared on standard *Drosophila* medium at 25°C. RNAi crosses and controls were performed at 29°C.

Molecular Biology

Torsin dsRNA was prepared by amplifying exon1 by PCR and in vitro transcribed using the Ambion MEGAscript T7 kit.

S2 Cell Culture and dsRNA Treatment

Drosophila SL2-NP2 cells were cultured and treated as described in Koles et al. (2012).

Immunocytochemistry

Third-instar larval body wall muscles were dissected and fixed as described in Budnik et al. (1996).

Antibody Generation

Anti-MAGI was generated by immunizing rats with a bacterially produced Magi peptide (amino acids 337–558).

Fluorescence In Situ Hybridization

Procedures for FISH were as described in Speese et al. (2012)

Transmission Electron Microscopy

TEM was performed as described in Ashley et al. (2005).

Diaminobenzidine conversion of Mini-SOG

Diaminobenzidine (DAB) photoconversion was adapted from Grabham and Goldberg (1997).

Image Acquisition

Confocal images were acquired using a Zeiss LSM700 confocal microscope equipped with a Zeiss ×63 Plan-Apochromat 1.4 NA DIC oil-immersion objective.

Quantification

Categorization of DFz2C/LamC Foci at the Light Microscopy Level

For categorization of nuclear DFz2C/LamC foci, larval body wall muscle preparations were labeled with antibodies to DFz2C and LamC and the number of nuclei at muscle 6 (segments A2–A4) with foci of the following categories were counted and divided by the total number of nuclei. A focus was considered "normal" if it contained a DFz2C spot localized within a thickening of the lamina (Figure 1A), "with small DFz2C puncta" if small DFz2C puncta localized at the lamina but there was no observable thickening of the lamina at this site (Figure 1B), or "containing depleted foci" if a thickening of the lamina devoid of DFz2C signal was observed (Figure 1C).

Ultrastructural Categorization of megaRNPs

Micrographs of foci at 78,000–110,000X total magnification were examined and megaRNPs were categorized as "within INM invaginations" if they appeared as a granule or granule cluster surrounded by an INM invagination, as "with a collared neck" if the granule was located within an enlarged perinuclear space and tethered to the INM through an electron-dense neck, or as "amorphous" if the granule was larger than 250 nm.

Categorization of NE Associated FISH Signal

For determining the percentage of signal outside the lamina, the number of lamina-associated FISH puncta was subdivided into those that were present either on the nucleoplasmic or cytoplasmic side of the LamC-immunoreactive lamina.

Measurements of Postsynaptic Protein Levels

Normalized postsynaptic protein levels were determined as described in Ramachandran et al. (2009).

Quantification of Bouton and Ghost Bouton Number

Bouton and ghost bouton numbers were assessed as described in Speese et al. (2012).

Statistical Analysis

See Extended Experimental Procedures for complete statistical analysis.

SUPPLEMENTAL INFORMATION

Supplemental Information includes four figures and Extended Experimental Procedures and can be found with this article online at http://dx.doi.org/10.1016/j.celrep.2013.03.015.

LICENSING INFORMATION

ACKNOWLEDGMENTS

We thank Drs. Xandra Breakefield, Mary Munson, Reid Gilmore, Emiliano Ricci, and members of the Budnik lab for helpful comments on the manuscript and discussions. We would like to thank the University of Massachusetts Medical School Electron Microscopy Facility for support in our ultrastructural studies and the Vienna Drosophila RNAi facility for providing the Torsin-RNAi line. We also thank Drs. Pamela Gayer, Yosef Gruenbaum, Georg Krohne, and Gertrud Schupbach for the generous gift of antibodies. This work was supported by National Institutes of Health grant R01 NS063228 (to V.B.). M.J.M. is a Howard Hughes Medical Institute investigator. V.J. carried out most of the experiments and contributed intellectually to the project. J.A. carried out some of the ultrastructural studies and contributed intellectually to the project and manuscript writing. J.N. carried out most the ultrastructural experiments. A.N. performed supporting FISH in wild-type and mutant larvae. N.I. and N.W.-I. provided the unpublished Torsin$^{\Delta E}$ fly strain and contributed to discussions. M.J.M. provided critical intellectual input and helped write the manuscript. V.B. directed the project and wrote the manuscript.

Received: January 4, 2013
Revised: March 11, 2013
Accepted: March 12, 2013
Published: April 11, 2013

REFERENCES

Ashley, J., Packard, M., Ataman, B., and Budnik, V. (2005). Fasciclin II signals new synapse formation through amyloid precursor protein and the scaffolding protein dX11/Mint. J. Neurosci. *25*, 5943–5955.

Ataman, B., Ashley, J., Gorczyca, D., Gorczyca, M., Mathew, D., Wichmann, C., Sigrist, S.J., and Budnik, V. (2006). Nuclear trafficking of Drosophila Frizzled-2 during synapse development requires the PDZ protein dGRIP. Proc. Natl. Acad. Sci. USA *103*, 7841–7846.

Ataman, B., Ashley, J., Gorczyca, M., Ramachandran, P., Fouquet, W., Sigrist, S.J., and Budnik, V. (2008). Rapid activity-dependent modifications in synaptic structure and function require bidirectional Wnt signaling. Neuron *57*, 705–718.

Barco, A., Lopez de Armentia, M., and Alarcon, J.M. (2008). Synapse-specific stabilization of plasticity processes: the synaptic tagging and capture hypothesis revisited 10 years later. Neurosci. Biobehav. Rev. *32*, 831–851.

Breakefield, X.O., Blood, A.J., Li, Y., Hallett, M., Hanson, P.I., and Standaert, D.G. (2008). The pathophysiological basis of dystonias. Nat. Rev. Neurosci. *9*, 222–234.

Budnik, V., Koh, Y.H., Guan, B., Hartmann, B., Hough, C., Woods, D., and Gorczyca, M. (1996). Regulation of synapse structure and function by the Drosophila tumor suppressor gene dlg. Neuron *17*, 627–640.

Goodchild, R.E., Kim, C.E., and Dauer, W.T. (2005). Loss of the dystonia-associated protein torsinA selectively disrupts the neuronal nuclear envelope. Neuron *48*, 923–932.

Grabham, P.W., and Goldberg, D.J. (1997). Nerve growth factor stimulates the accumulation of beta1 integrin at the tips of filopodia in the growth cones of sympathetic neurons. J. Neurosci. *17*, 5455–5465.

Grünwald, D., Singer, R.H., and Rout, M. (2011). Nuclear export dynamics of RNA-protein complexes. Nature *475*, 333–341.

Iyer, L.M., Leipe, D.D., Koonin, E.V., and Aravind, L. (2004). Evolutionary history and higher order classification of AAA+ ATPases. J. Struct. Biol. *146*, 11–31.

Kim, C.E., Perez, A., Perkins, G., Ellisman, M.H., and Dauer, W.T. (2010). A molecular mechanism underlying the neural-specific defect in torsinA mutant mice. Proc. Natl. Acad. Sci. USA *107*, 9861–9866.

Köhler, A., and Hurt, E. (2007). Exporting RNA from the nucleus to the cytoplasm. Nat. Rev. Mol. Cell Biol. *8*, 761–773.

Koles, K., Nunnari, J., Korkut, C., Barria, R., Brewer, C., Li, Y., Leszyk, J., Zhang, B., and Budnik, V. (2012). Mechanism of evenness interrupted (Evi)-exosome release at synaptic boutons. J. Biol. Chem. *287*, 16820–16834.

Maric, M., Shao, J., Ryan, R.J., Wong, C.S., Gonzalez-Alegre, P., and Roller, R.J. (2011). A functional role for TorsinA in herpes simplex virus 1 nuclear egress. J. Virol. *85*, 9667–9679.

Mathew, D., Ataman, B., Chen, J., Zhang, Y., Cumberledge, S., and Budnik, V. (2005). Wingless signaling at synapses is through cleavage and nuclear import of receptor DFrizzled2. Science *310*, 1344–1347.

Mettenleiter, T.C., Klupp, B.G., and Granzow, H. (2006). Herpesvirus assembly: a tale of two membranes. Curr. Opin. Microbiol. *9*, 423–429.

Naismith, T.V., Heuser, J.E., Breakefield, X.O., and Hanson, P.I. (2004). TorsinA in the nuclear envelope. Proc. Natl. Acad. Sci. USA *101*, 7612–7617.

Neuwald, A.F., Aravind, L., Spouge, J.L., and Koonin, E.V. (1999). AAA+: A class of chaperone-like ATPases associated with the assembly, operation, and disassembly of protein complexes. Genome Res. *9*, 27–43.

Ozelius, L.J., Hewett, J.W., Page, C.E., Bressman, S.B., Kramer, P.L., Shalish, C., de Leon, D., Brin, M.F., Raymond, D., Corey, D.P., et al. (1997). The early-onset torsion dystonia gene (DYT1) encodes an ATP-binding protein. Nat. Genet. *17*, 40–48.

Packard, M., Koo, E.S., Gorczyca, M., Sharpe, J., Cumberledge, S., and Budnik, V. (2002). The Drosophila Wnt, wingless, provides an essential signal for pre- and postsynaptic differentiation. Cell *111*, 319–330.

Ramachandran, P., Barria, R., Ashley, J., and Budnik, V. (2009). A critical step for postsynaptic F-actin organization: regulation of Baz/Par-3 localization by aPKC and PTEN. Dev. Neurobiol. *69*, 583–602.

Richter, J.D. (2001). Think globally, translate locally: what mitotic spindles and neuronal synapses have in common. Proc. Natl. Acad. Sci. USA *98*, 7069–7071.

Ruiz-Canada, C., Ashley, J., Moeckel-Cole, S., Drier, E., Yin, J., and Budnik, V. (2004). New synaptic bouton formation is disrupted by misregulation of microtubule stability in aPKC mutants. Neuron *42*, 567–580.

Shu, X., Lev-Ram, V., Deerinck, T.J., Qi, Y., Ramko, E.B., Davidson, M.W., Jin, Y., Ellisman, M.H., and Tsien, R.Y. (2011). A genetically encoded tag for correlated light and electron microscopy of intact cells, tissues, and organisms. PLoS Biol. *9*, e1001041.

Speese, S.D., Ashley, J., Jokhi, V., Nunnari, J., Barria, R., Li, Y., Ataman, B., Koon, A., Chang, Y.-T., Li, Q., et al. (2012). Nuclear envelope budding enables large ribonucleoprotein particle export during synaptic Wnt signaling. Cell *149*, 832–846.

Tanabe, L.M., Kim, C.E., Alagem, N., and Dauer, W.T. (2009). Primary dystonia: molecules and mechanisms. Nat. Rev. Neurol. *5*, 598–609.

Wakabayashi-Ito, N., Doherty, O.M., Moriyama, H., Breakefield, X.O., Gusella, J.F., O'Donnell, J.M., and Ito, N. (2011). Dtorsin, the Drosophila ortholog of the early-onset dystonia TOR1A (DYT1), plays a novel role in dopamine metabolism. PLoS ONE *6*, e26183.

Walker, J.E., Saraste, M., Runswick, M.J., and Gay, N.J. (1982). Distantly related sequences in the alpha- and beta-subunits of ATP synthase, myosin, kinases and other ATP-requiring enzymes and a common nucleotide binding fold. EMBO J. *1*, 945–951.

Wiersma-Meems, R., Van Minnen, J., and Syed, N.I. (2005). Synapse formation and plasticity: the roles of local protein synthesis. Neuroscientist *11*, 228–237.

SUPPORTING DATA:

Pathway	gene	function	RNAi line	Modification
Dopamine signaling	Pu	GTP cyclohydrolase/dopamine synthesis	KK107963	**E+++**
	DAT	dopamine transporter/dopamine pool	KK10046	**S+++**
	DopR2	dopamine D1 receptor/dopamine signaling	JF02043	**S+++**
	D2R	dopamine D2 receptor/dopamine signaling	JF02025	**E+++**
	Gαs	G protein α s subunit/dopamine signaling	JF03255	**S+++**
	Gαq	G protein α q subunit/dopamine signaling	JF02464	**E+++**
	Gαi	G protein α i subunit/dopamine signaling	JF01608	**E+++**
RNP transport	Lamin C	Nuclear RNP exit	JF01406	E++
	par6	Nuclear RNP exit	HMS01410	E++
	aPKC	Nuclear RNP exit	HMS01320	E+
	baz	Nuclear RNP exit	JF01079	E+
	stau	RNP transport	JF01764	E++
	Fmr1	RNP transport	HMS00248	E++
Axon guidance/cell migration	Fas2	cell adhesion/axon guidance	HMS01098	**E+++**
	robo	axon guidance	HMS01517	**S+++**
	leak/robo2	axon guidance	HMS01063	**S+++**
	slit	axon guidance	JF01228	**S+++**
	shg	DE cadherin/cell migration	HMS00693	**S+++**
	Dwnt5	axon guidance	HMS01119	**E+++**

Table 1. Candidate modifier genes of *dtorsin*-null locomotion phenotype. E+++: strong enhancer (peristaltic rates $25 \leq x \leq 35$, $p<0.0001$), E++: moderately strong enhancer, E+: weak enhancer. S+++: strong suppressor (peristaltic rates $50 \leq x \leq 60$, $p<0.0001$).

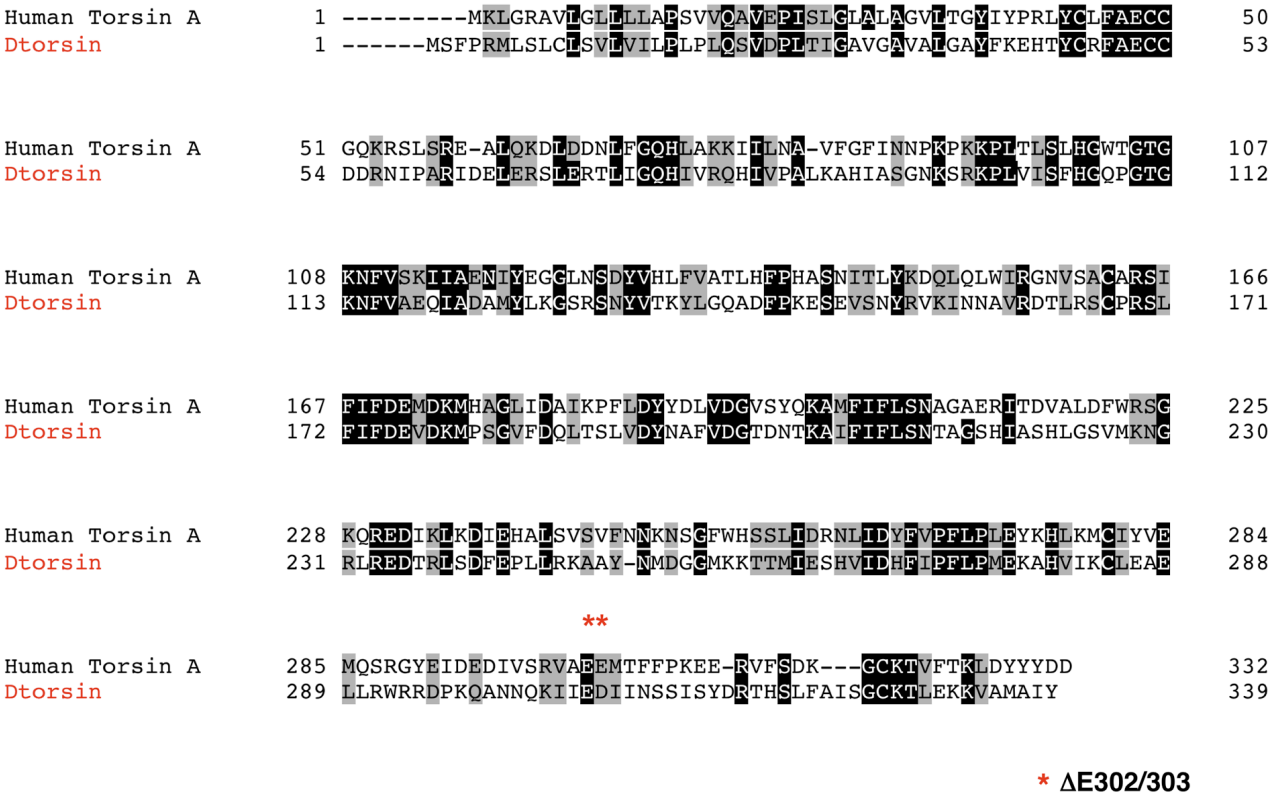

Figure 1. Alignment of human torsinA and *Drosophila* Dtorsin protein sequences. Human torsinA (AAC51732) and *Drosophila dtorsin* (Torsin) (NP_572178) amino acid sequences were aligned using DNA strider (version 1.4f19). Two possible locations of a single glutamate deletion (ΔE302 or ΔE303) are indicated by red asterisks. Identical amino acids are marked by black boxes. Conserved amino acids are marked by gray boxes.

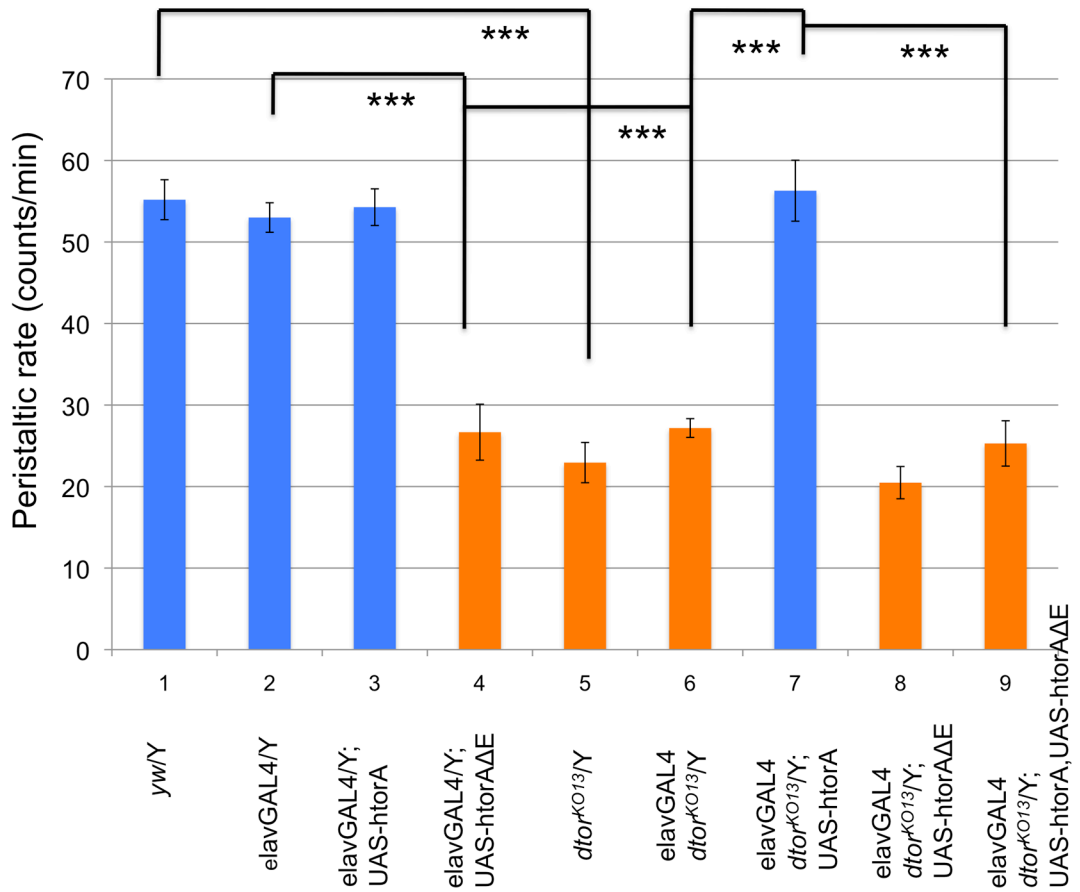

Figure 2. Neuronal expression of human torsinAΔE has a dominant-negative effect on larval locomotion. Peristaltic frequencies were counted for the wandering stage third instar larvae of the genotype: (1) *y w*/Y (wild type) male (n=15), (2) *w elavGAL4*/Y (wild type) male (n=9), (3) *w elavGAL4*/Y; UAS-htorsinA/+ male (n=15), (4) *w elavGAL4*/Y; UAS-htorsinAΔE/+ male (n=9), (5) *y w dtorsin*^{KO13}/Y (*dtorsin*-null) male (n=14), (6) *w elavGAL4 dtorsin*^{KO13}/Y (*dtorsin*-null) male (n=39), (7) *w elavGAL4 dtorsin*^{KO13}/Y; UAS-htorsinA/+ male (n=14), (8) *w elavGAL4 dtorsin*^{KO13}/Y; UAS-htorsinAΔE/+ male (n=21), (9) *w elavGAL4 dtorsin*^{KO13}/Y; UAS-htorsinA, UAS-htorsinAΔE/+ male (n=14). Results are expressed as the mean ± S.E.M. *** p<0.0001.

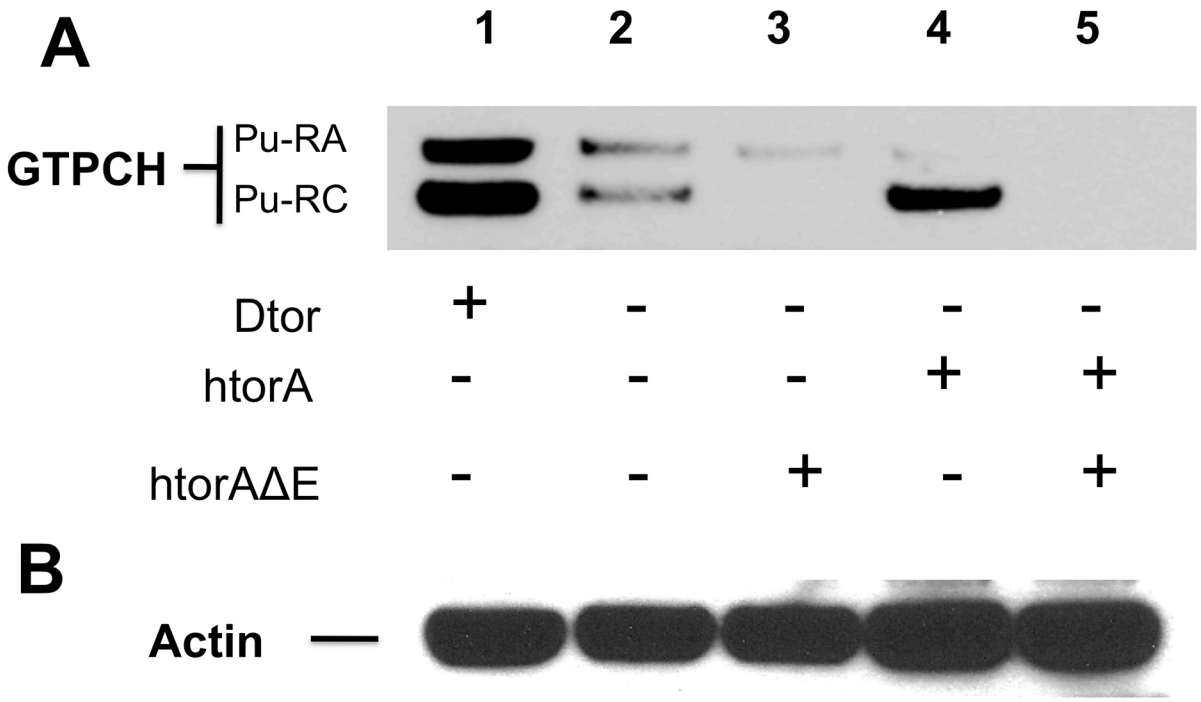

Figure 3. Neuronal expression of human torsinAΔE has a dominant-negative effect on GTPCH protein levels in adult brains. Adult head extracts were analyzed by Western blots. The membrane was probed with anti-GTPCH A/C (upper panel) and reprobed with anti-actin (lower panel). The genotypes are: (1) *y w*/Y (wild type) males, (2) *y w dtorsin*^{KO13}/Y (*dtorsin*-null) males, (3) *w elavGAL4 dtorsin*^{KO13}/Y; UAS-htorsinAΔE/+ males, (4) *w elavGAL4 dtorsin*^{KO13}/Y; UAS-htorsinA/+ males, (5) *w elavGAL4 dtorsin*^{KO13}/Y; UAS-htorsinA, UAS-htorsinAΔE/+ males. The locations of GTPCH (Pu-RA: 45 kDa, Pu-RC: 43 kDa) and actin (42 kDa) are indicated. Thirty μg of proteins were loaded in each lane.

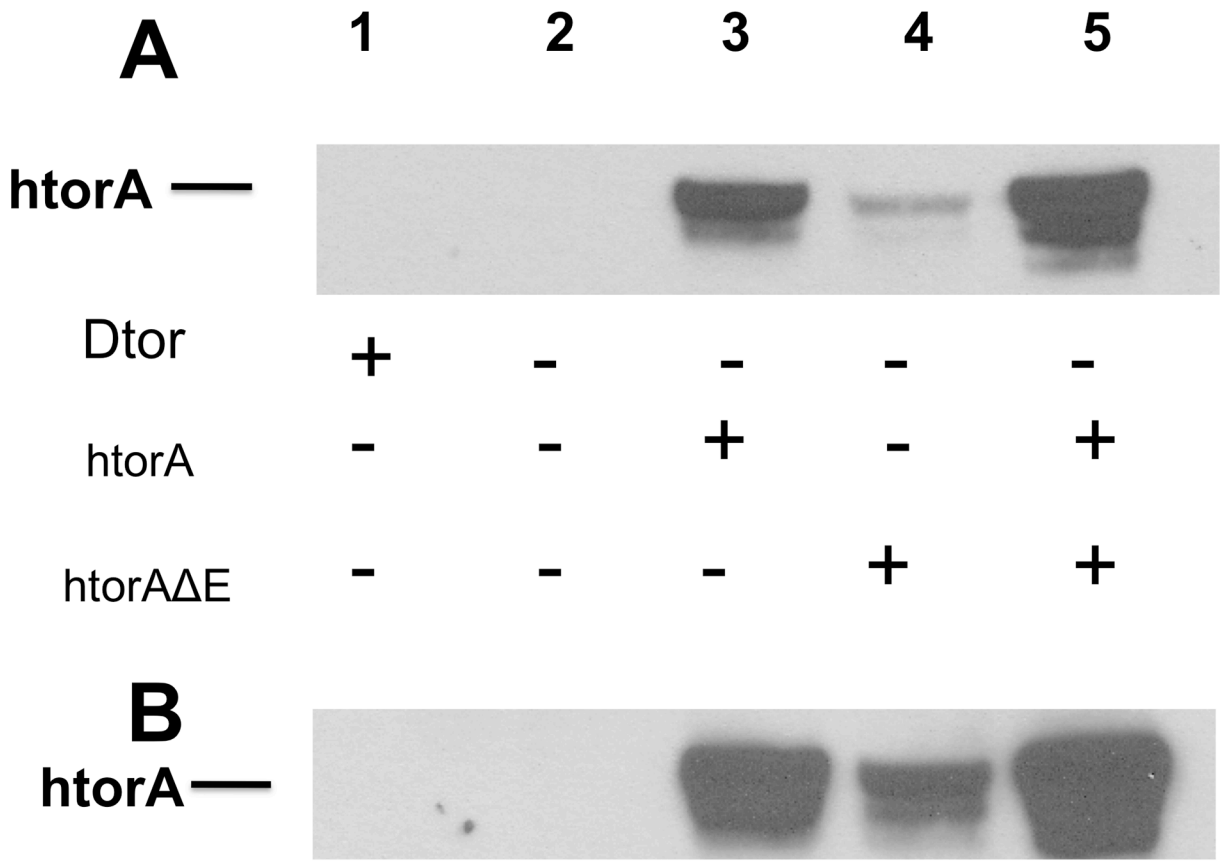

Figure 4. Expression of human torsinA protein in adult heads driven by the pan-neuronal elavGAL4. A. Adult head extracts were analyzed by Western blots. The membrane was probed with rabbit anti-human torsinA. The genotypes are: (1) *y w*/Y (wild type) males, (2) *dtorsin*^{KO13}/Y (*dtorsin*-null) males, (3) *w elavGAL4 dtorsin*^{KO13}/Y; UAS-htorsinA/+ males, (4) *w elavGAL4 dtorsin*^{KO13}/Y; UAS-htorsinAΔE/+ males, (5) *w elavGAL4 dtorsin*^{KO13}/Y; UAS-htorsinA, UAS-htorsinAΔE/+ males. The location of human torsinA (37 kDa) is indicated. Thirty µg of proteins were loaded in each lane. **B.** A longer exposure of the same blot as in A to demonstrate that human torsinAΔE is expressed in lane 4, although it is at a much lower level.

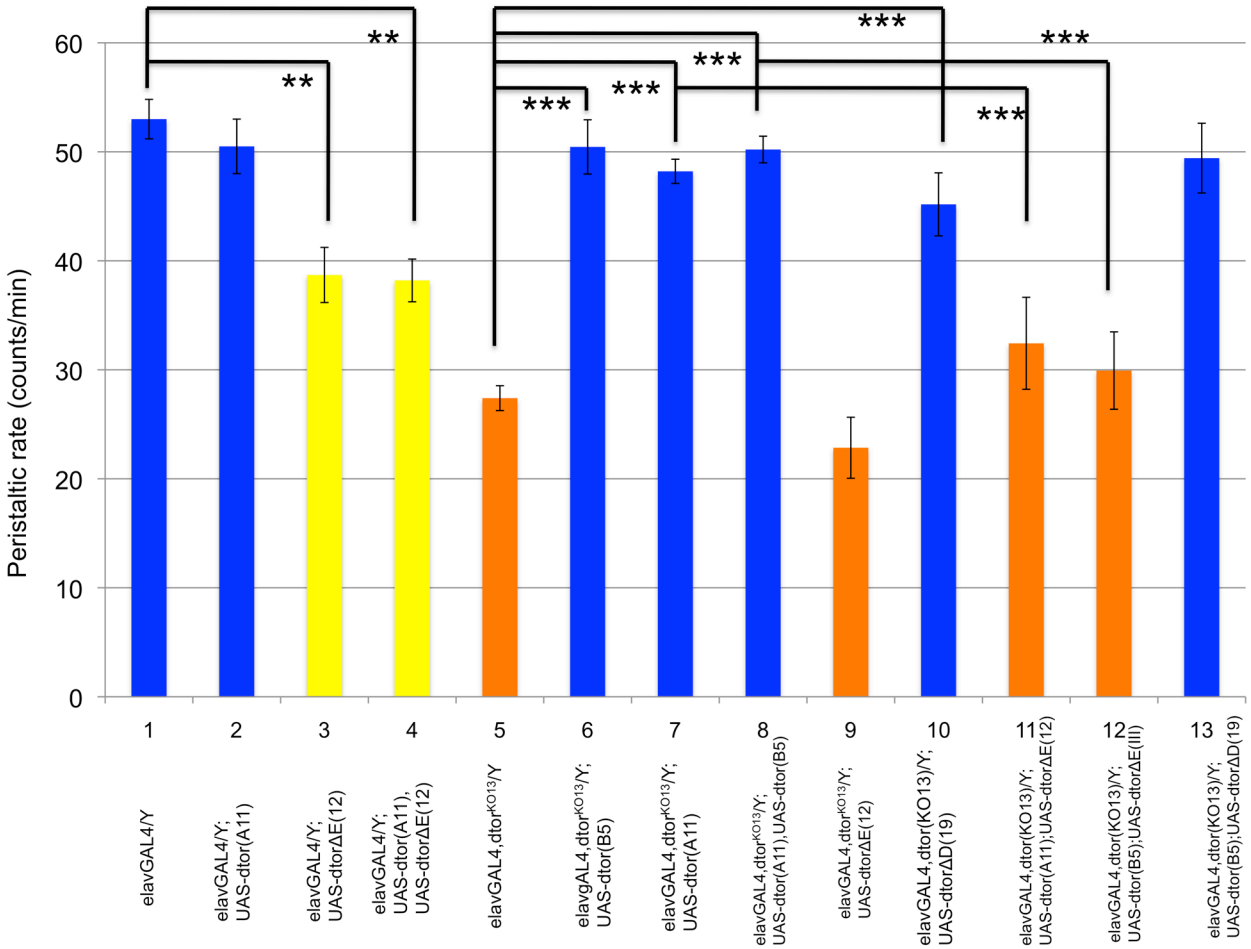

Figure 5. Neuronal expression of *Drosophila* DtorsinΔE has a dominant-negative effect on larval locomotion. Peristaltic frequencies were counted for the wandering stage third instar larvae of the genotype: (1) *w elavGAL4*/Y (wild type) male (n=9), (2) *w elavGAL4*/Y; UAS-*dtorsin*(A11)(III)/+ male (n=8), (3) *w elavGAL4*/Y; UAS-*dtorsin*ΔE(#12)(II)/+ male (n=23), (4) *w elavGAL4*/Y; UAS-*dtorsin*ΔE(#12)(II)/+; UAS-*dtorsin*(A11)(III)/+ male (n=15), (5) *w elavGAL4 dtorsin*^{KO13}/Y (*dtorsin*-null) male (n=48), (6) *w elavGAL4 dtorsin*^{KO13}/Y; UAS-*dtorsin*(B5)(II)/+ male (n=20), (7) *w elavGAL4 dtorsin*^{KO13}/Y; UAS-*dtorsin*(A11)(III)/+ male (n=9), (8) *w elavGAL4 dtorsin*^{KO13}/Y; UAS-*dtorsin*(B5)(II)/+; UAS-*dtorsin*(A11)(III)/+ male (n=23), (9) *w elavGAL4 dtorsin*^{KO13}/Y; UAS-*dtorsin*ΔE(#12)(II)/+ male (n=13), (10) *w elavGAL4 dtorsin*^{KO13}/Y; UAS-*dtorsin*ΔD/+ male (n=11), (11) *w elavGAL4 dtorsin*^{KO13}/Y; UAS-*dtorsin*(A11)(III)/+; UAS-*dtorsin*ΔE(#12)(II)/+ male (n=7), (12) *w elavGAL4 dtorsin*^{KO13}/Y; UAS-*dtorsin*(B5)(II)/+; UAS-*dtorsin*ΔE(#21)(III)/+ male (n=14), (13) *w elavGAL4 dtorsin*^{KO13}/Y; UAS-*dtorsin*(B5)(II)/+; UAS-*dtorsin*ΔD/+ male (n=20). Results are expressed as the means ± S.E.M. *** p<0.0001. ** p<0.001.

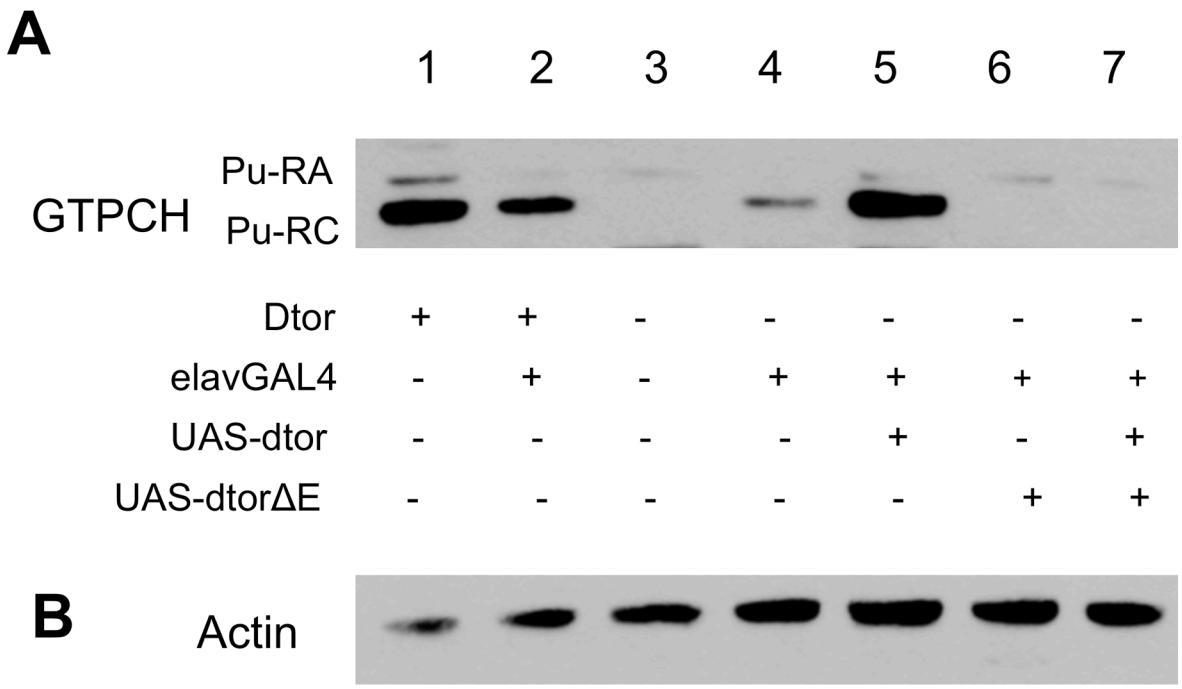

Figure 6. Neuronal expression of *Drosophila* DtorsinΔE has a dominant-negative effect on GTPCH protein levels. Adult head extracts were analyzed by Western blots. The membrane was probed with anti-GTPCH A/C (upper panel) and reprobed with anti-actin (lower panel). The genotypes are: (1) *y w*/Y (wild type) males, (2) *w elavGAL4*/Y (wild type) males, (3) *y w dtorsin*^{KO13}/Y (*dtorsin*-null) males, (4) *w elavGAL4 dtorsin*^{KO13}/Y (*dtorsin*-null) males, (5) *w elavGAL4 dtorsin*^{KO13}/Y; UAS-*dtorsin*(B5)(II)/+ males, (6) *w elavGAL4 dtorsin*^{KO13}/Y; UAS- *dtorsinΔE*(#12)(III)/+ males, (7) *w elavGAL4 dtorsin*^{KO13}/Y; UAS-*dtorsin*(B5)(II): UAS-*dtorsin*ΔE(#12)(III)/+ males. The locations of GTPCH (Pu-RA: 45 kDa, Pu-RC: 43 kDa) and actin (42 kDa) are indicated. Thirty μg of proteins were loaded in each lane.

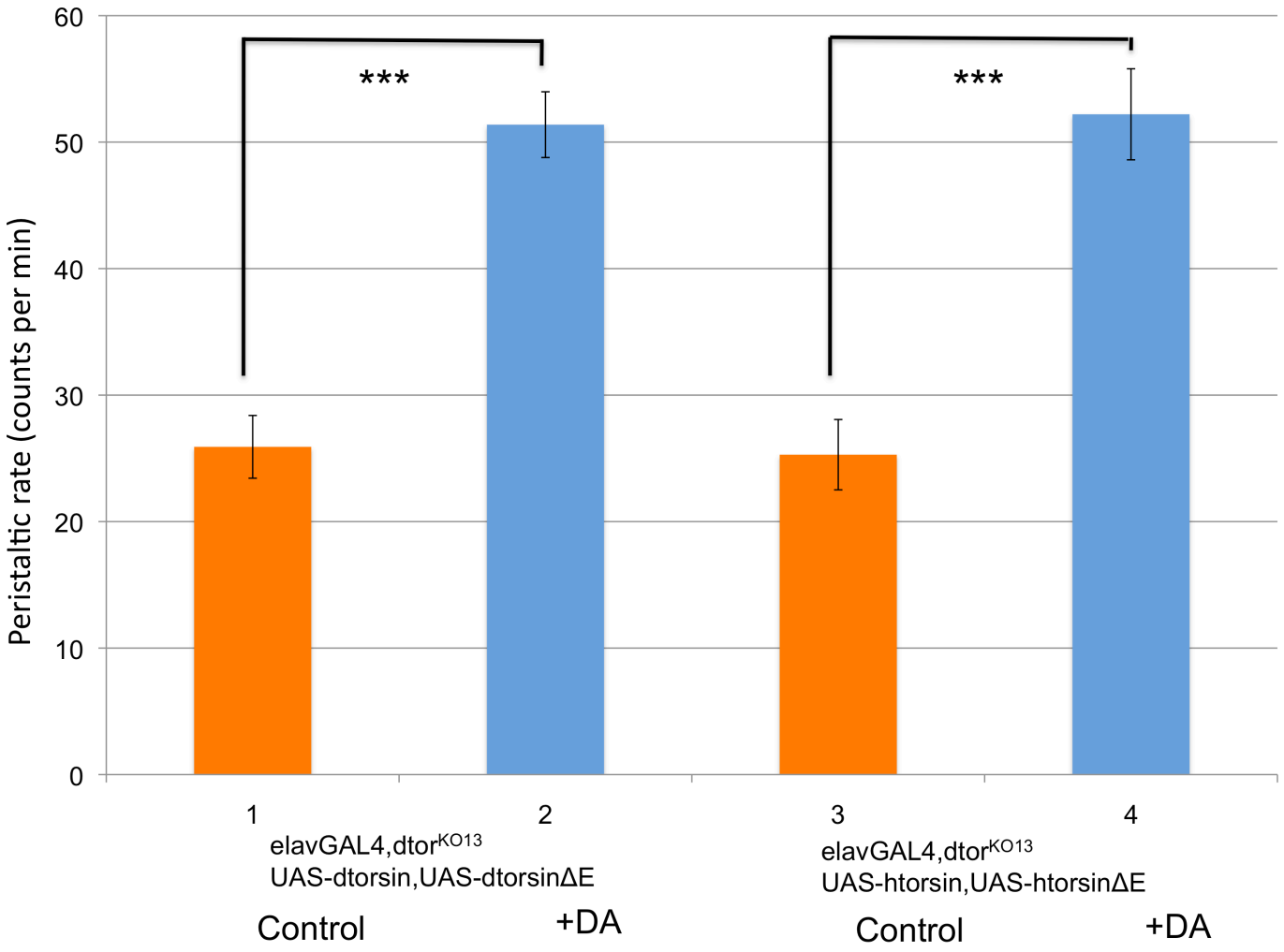

Figure 7. Larval locomotion defects caused by neuronal expression of *Drosophila* DtorsinΔE or human torsinAΔE can be rescued by dopamine supplementation. Peristaltic frequencies were counted for the wandering stage third instar larvae. The genotypes are: (1) *w elavGAL4 dtorsin*^{KO13}/Y; UAS-*dtorsin*ΔE(#12)(II)/+; UAS-*dtorsin*(A11)(III)/+ males without dopamine supplementation (n=11), (2) *w elavGAL4 dtorsin*^{KO13}/Y; UAS-*dtorsin*ΔE(#12)(II)/+; UAS-*dtorsin*(A11)(III)/+ males with 20 mM dopamine supplementation (n=8), (3) *w elavGAL4 dtorsin*^{KO13}/Y; UAS-htorsinA, UAS-htorsinΔE/+ males without dopamine supplementation (n=14), (4) *w elavGAL4 dtorsin*^{KO13}/Y; UAS-htorsinA, UAS-htorsinΔE/+ males with 20 mM dopamine supplementation (n=5). Results are mean ± S.E.M. *** $p<0.0001$, very significant difference between without and with 20 mM dopamine supplementation.

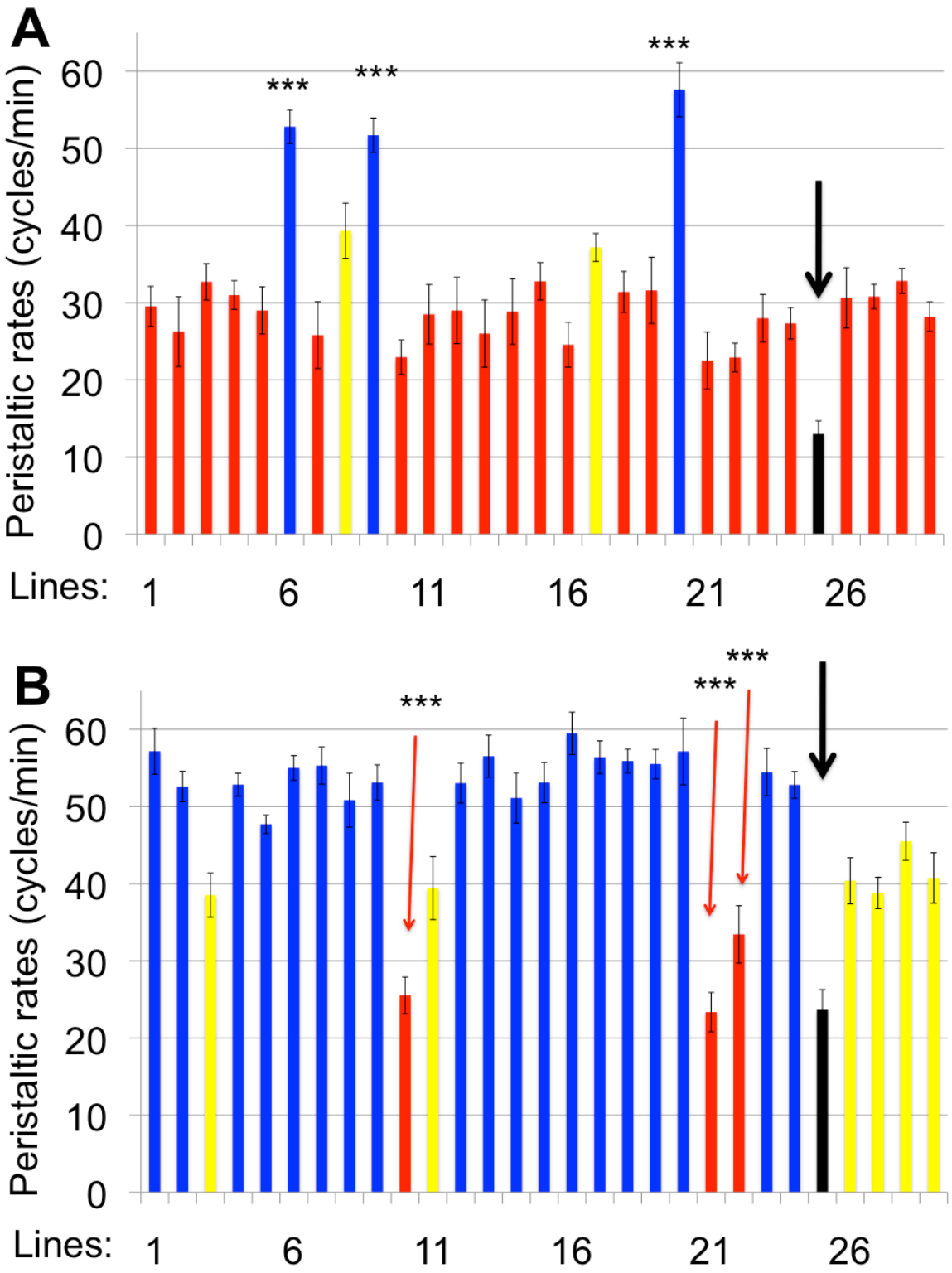

Figure 8. Modification of *dtorsin*-null locomotion defects by neuronal RNAi expression. A. *dtorsin*-null hemizygotes (elavGAL4, *dtorsin*-null/Y; UAS-RNAi) B. *dtorsin*-null heterozygotes (elavGAL4/+; UAS-RNAi) 1: no RNAi. 2-29: RNAi line #2-#29. Y-axis: peristaltic rates. *** $p<0.0001$